Regeneration in the adult *Drosophila* brain

Kassi L. Crocker[1,2,3], Khailee Marischuk[1,3], Stacey A. Rimkus[3#], Hong Zhou[4], Jerry C.P. Yin[4] and Grace Boekhoff-Falk[1,3*]
[1]Genetics Graduate Training Program
[2]Science and Medicine Graduate Research Scholars Program
[3]Department of Cell and Regenerative Biology
[4]Department of Genetics
University of Wisconsin-Madison
School of Medicine and Public Health
1111 Highland Avenue
Madison, WI 53705

[#]current address: Laboratory of Genetics, University of Wisconsin-Madison 53706

*corresponding author
Tel: 608-262-1609
Fax: 608-262-7306
Email: grace.boekhoff@wisc.edu

52 **Abstract**

53 Neurodegenerative diseases such as Alzheimer's and Parkinson's currently affect ~25 million
54 people worldwide (ERKKINEN *et al.* 2018). The global incidence of traumatic brain injury (TBI) is
55 estimated at ~70 million/year (DEWAN *et al.* 2018). Both neurodegenerative diseases and TBI
56 remain without effective treatments. We are utilizing adult *Drosophila melanogaster* to
57 investigate the mechanisms of brain regeneration with the long term goal of identifying targets
58 for neural regenerative therapies. Like mammals, Drosophila have few proliferating cells in the
59 adult brain. Nonetheless, within 24 hours of a Penetrating Traumatic Brain Injury (PTBI) to the
60 central brain, there is a significant increase in the number of proliferating cells. We subsequently
61 detect both new glia and new neurons and the formation of new axon tracts that target
62 appropriate brain regions. Glial cells divide rapidly upon injury to give rise to new glial cells.
63 Other cells near the injury site upregulate neural progenitor genes including *asense* and
64 *deadpan* and later give rise to the new neurons. Locomotor abnormalities observed after PTBI
65 are reversed within two weeks of injury, supporting the idea that there is functional recovery.
66 Together, these data indicate that adult *Drosophila* brains are capable of neuronal repair. We
67 anticipate that this paradigm will facilitate the dissection of the mechanisms of neural
68 regeneration and that these processes will be relevant to human brain repair.

69 **Introduction**

70 Although classical studies reported that the mammalian brain stops making new neurons shortly
71 after birth (RAMON Y CAJAL 1913; RAMON Y CAJAL 1914), populations of dividing progenitor cells
72 subsequently were observed in two major regions of the rodent brain: the subventricular zone
73 (SVZ) of the forebrain and the dentate gyrus (DG) of the hippocampus (ALTMAN AND DAS 1965;
74 ALTMAN 1969; KAPLAN AND HINDS 1977). Both SVZ and DG progenitors give rise to multiple cell
75 types over the course of an animal's lifetime, including neurons, astrocytes and
76 oligodendrocytes (KUHN *et al.* 1996). Moreover, a landmark study published in 1998 concluded
77 that adult humans create new neurons in the hippocampus in the absence of injury (ERIKSSON
78 *et al.* 1998).

79 The discovery of adult neurogenesis raised the possibility of utilizing endogenous cells
80 for neural regeneration both following brain injury and also in patients suffering from
81 neurodegenerative diseases. Although emphasis in the mammalian neural regeneration field to
82 date has been on transplanting embryonic or induced pluripotent stem cells (VISHWAKARMA *et*
83 *al.* 2014), obtaining functional integration of transplanted neural cells remains a major challenge.
84 Moreover, stem cell transplants can be accompanied by tumor formation (AMARIGLIO *et al.*
85 2009). A more recent direction for the field therefore has been on coaxing resident cells in the
86 brain to undertake regeneration (GAO *et al.* 2016).

87 In order to utilize endogenous cells for neural repair in clinical settings, we first must
88 identify the cell types and underlying molecular mechanisms that contribute to
89 neuroregeneration. To address these questions, we are investigating repair of the adult brain in
90 the fruitfly *Drosophila melanogaster.* The adult *Drosophila* brain, like the adult mammalian
91 brain, has few proliferative cells (VON TROTHA *et al.* 2009). In addition, although the *Drosophila*
92 brain has many fewer neurons, the *Drosophila* brain has many shared complexities with the
93 human brain including analogous neural cell types (LESSING AND BONINI 2009), common
94 neurotransmitters (GABA, glutamate, and acetylcholine) (BELLEN *et al.* 2010), similar synapse

architecture (LESSING AND BONINI 2009) and similar physiology and intracellular signaling pathways (BELLEN *et al.* 2010). These properties, combined with a wealth of genetic and molecular tools, a short generation time, and large number of offspring, lead us to propose that *Drosophila* offer an exceptional model in which to investigate brain regeneration.

The combination of rare cell proliferation and the fact that known neural progenitors undergo terminal differentiation or apoptosis during metamorphosis (SIEGRIST *et al.* 2010), make it all the more remarkable that the adult *Drosophila* brain is capable of neurogenesis. Nonetheless, the adult *Drosophila* brain can make new neurons after injury (FERNANDEZ-HERNANDEZ *et al.* 2013; MORENO *et al.* 2015). These earlier studies focused on the adult optic lobes, where slowly cycling neural progenitor cells were discovered in the medulla cortex. These progenitors are activated by injury and give rise to new neurons (FERNANDEZ-HERNANDEZ *et al.* 2013; MORENO *et al.* 2015).

Here, in contrast to other studies, we focus on a distinct brain region, the central brain. We find that the central brain, like the optic lobes, can produce new neurons after injury. However, in contrast to the optic lobes, the new central brain neurons innervate specific targets, including the mushroom body, ellipsoid body, antennal lobes and lateral horn. We present evidence that these new neurons contribute to functional regeneration. Also, in contrast to the optic lobes, the central brain produces new glial cells in response to injury. We have lineage-traced both the new neurons and the new glia and find that they arise from distinct progenitors. We propose that an injury-triggered mechanism results in the reactivation of neural progenitor genes, allowing these cells to proliferate and give rise to new neurons. Because of the extensive parallels between adult Drosophila and mammalian brains, we anticipate that these studies will have relevance to human neural regeneration.

121 **Results**

122 Penetrating Traumatic Brain Injury (PTBI) stimulates cell proliferation

123 To investigate the regenerative capacity of the adult *Drosophila melanogaster* central brain, we
124 examined brains at a variety of time points following a penetrating traumatic brain injury (PTBI).
125 We injured the central brain near the mushroom body (MB; **Fig. 1A**) through the head cuticle
126 using a stainless steel insect pin (~12.5μm diameter tip, 100 μm diameter rod). This is the
127 same type of pin used by Fernandez-Hernandez *et al.* to injure adult brains (FERNANDEZ-
128 HERNANDEZ *et al.* 2013), but distinct from that used by Sanuki *et al*. (SANUKI *et al.* 2019) who
129 used larger (150 μm diameter), hollow, syringe needle**.** These earlier studies examined the
130 consequences of injury to the adult optic lobes. In contrast, we injured the adult central brain
131 near the mushroom body. Mushroom body neuroblasts are the last to stop proliferating during
132 development (ITO AND HOTTA 1992; ITO *et al.* 1997; SIEGRIST *et al.* 2010). We therefore
133 reasoned that the mushroom body might have residual mitotic potential. Located dorsally in the
134 central brain, the mushroom body is critical for learning and memory and contains complex
135 dendrite and axon arbors in highly stereotyped arrays (ASO *et al.* 2014).

136 One early hallmark of a regenerative response is cell proliferation (ZHOU *et al.* 2016). We
137 therefore tested whether PTBI stimulates proliferation, using two different assays. We first
138 utilized antibodies to the mitotic marker, phospho-histone H3 (PH3). Histone H3 is transiently
139 phosphorylated during M phase of the cell cycle (HANS AND DIMITROV 2001), and antibodies to
140 PH3 are often used to identify dividing cells. Within 24 hours of PTBI, brains from young adult
141 males exhibited a significant increase of PH3+ cells compared to uninjured controls of the same
142 sex, age, and genotype (**Fig. 1B-E, J**). We then wanted to determine whether these newly
143 created cells were maintained or eliminated. Because PH3 only transiently labels dividing cells,
144 we also used incorporation of the nucleotide analog 5-ethynyl-2'-deoxyuridine (EdU). EdU is
145 incorporated into newly synthesized DNA and therefore more permanently labels dividing cells
146 and their progeny. After feeding flies EdU for various lengths of time, we detected the

147 incorporated EdU using fluorescent ‘click chemistry’ (InVitrogen®). Consistent with the PH3
148 labeling at 24 hours, we observed 5- and 15-fold more EdU+ cells at 7 days and 14 days post-
149 injury, respectively, compared to uninjured controls (p-value<0.0001 and p-value<0.0002) (**Fig.**
150 **1F-J**). This indicates that cell proliferation continues between 7 and 14 days post-PTBI.
151 EdU permanently marks dividing cells and allows us to measure the cumulative number
152 of cells that had divided since the PTBI. In contrast, PH3 provides a snapshot of actively
153 dividing cells. To evaluate the dynamics of cell proliferation, we therefore compared mitotic
154 activity using anti-PH3 in animals at 24 hours, 7 days and 14 days post-PTBI (**Fig. S1A, E**).
155 Consistent with the EdU labeling experiments above, we observed actively dividing cells even
156 14 days post-injury, although the numbers of dividing cells decrease with time post-PTBI. To
157 test whether age impacts regenerative capacity, we aged adult males to 7, 14, and 28 days
158 post-eclosion prior to PTBI, then assayed for cell proliferation 24 hours later.
159 Adult male brains injured 7 days post- eclosion had significantly fewer PH3+ cells than
160 brains injured within 6 hours of eclosion (**Fig. S1B**). The brains injured at 7 days had more
161 PH3+ cells than the age-matched uninjured controls, but fewer PH3+ cells than brains injured
162 within 6 hours of eclosion (**Fig. S1B**). Brains injured at either 14 or 28 days post-eclosion
163 exhibited little cell proliferation that did not differ from age-matched uninjured controls (**Fig.**
164 **S1B**). Taken together, these data support the idea that early in adulthood, *Drosophila* brains
165 possess cells that can initiate division in response to injury and that this proliferative ability
166 declines with age.
167 The increase in EdU+ cells between 7 and 14 days post-PTBI (**Fig. 1J**) and the
168 presence of actively dividing, PH3+ cells at 7 and 14 days post-PTBI (**Fig. S1A**) indicate that the
169 capacity for sustained cell proliferation is retained beyond the time window during which cell
170 proliferation can be initiated. In other words, once adult brain cells begin to divide, they may
171 continue to divide for up to 2 weeks. However, by 2 weeks of adulthood, brain cells no longer
172 can be stimulated by injury to divide. Of note, uninjured flies at both 24 hours and 7 days exhibit

173 similar baseline cell proliferation (**Fig. S1B**). Taken together, this indicates that the presence of
174 PH3+ cells in uninjured brains does not correlate directly with the brain's regenerative potential.
175 Pulse-chase experiments allowed us to test whether the cells incorporating EdU were
176 viable; if a cell dies after synthesizing DNA, the incorporated EdU is expected to be either
177 diffuse or punctate instead of uniformly distributed within each labeled nucleus. There were
178 similar numbers of labeled nuclei in brains from animals either pulse-chase or continuously fed
179 EdU (**Fig. S1C**). This indicates that most EdU-labeled cells survive. Interestingly, at later
180 timepoints post-PTBI, there was a statistically significant increase in the number of EdU-positive
181 cells not only in the injured brain hemisphere, but also in the contralateral, uninjured brain
182 hemisphere (**Fig. S1D**). This indicates that PTBI may induce both local and widespread
183 proliferation. For this reason, we use brains from uninjured animals as controls instead of the
184 contralateral, uninjured brain hemispheres.
185
186 <u>Characterizing the identities of dividing cells post-injury</u>
187 To determine the identities of the mitotically active cells, we fed young adult males with EdU,
188 then simultaneously assayed for EdU incorporation, expression of the glial protein Reversed
189 polarity (Repo) and expression of the neuronal protein Embryonic lethal, abnormal vision (Elav).
190 At 7 days post-injury, we observed 4 classes of cells (**Fig. 2A-D'''**): cells that were EdU+ but did
191 not express either Elav or Repo (arrowheads in **Fig. 2A-A'''**; Class I); cells that were EdU+ and
192 Repo+, i.e. glia (arrowheads in **Fig. 2B-B'''**; Class II); cells that were EdU+ and express Elav,
193 i.e. neurons (arrowheads in **Fig. 2C-C'''**; Class III); and cells that were EdU+, Repo+, and Elav+
194 (arrowheads in **Fig. 2D-D'''**; Class IV). These data indicate that cells actively divide after PTBI,
195 and that the dividing cells either are, or become, glia and neurons.
196 As described above, age plays an important role in the proliferative capacity of brain
197 cells. We therefore asked whether the amount of time after injury impacts the identities of
198 proliferating cells. Specifically, we compared the ratios of proliferating cells in each of the 4

199 classes at 24 hours, 7 days and 14 days post-PTBI. (**Fig. 2F**). The proliferation marker we used
200 in the 24-hour assay was anti-PH3, while the marker used in the 7 and 14 day assays was EdU
201 incorporation. At 24 hours post-injury, we observed the following distribution of classes: 56%
202 Class I (PH3+); 38% Class II (PH3+Repo+); and 5% Class IV (PH3+Repo+Elav+) (**Fig. 2F**).
203 Significantly, at 24 hours post-PTBI, there are no Class III (PH3+Elav+) cells (**Fig. 2F**). By 7
204 days post-PTBI, 13% of the EdU+ cells are Class III, i.e. new neurons (**Fig. 2F**). By 14 days
205 post-PTBI, 29% of the EdU+ cells are new neurons (**Fig. 2F**). Also, by 14 days post-PTBI, there
206 are no longer any Class IV cells that express a hybrid glial and neuronal identity. Of
207 significance, neither Class IV cells, nor the Class III adult-generated neurons are detected in
208 uninjured adult brains at any of the three timepoints (**Fig. 2E)**. Also, although the ratios of Class
209 I to Class II cells are similar in uninjured and injured brains, the total numbers of dividing cells
210 are quite different. 24 hour control brains averaged 2.5 dividing cells/brain (11 brains; 28 PH3+
211 cells) compared to 10.7 dividing cells/brain following PTBI (17 brains; 181 PH3+ cells). At 7
212 days, control brains averaged 1.7 EdU+ cell/brain (9 brains; 15 dividing cells) compared to 11.5
213 EdU+ cells/brain following PTBI (15 brains; 172 EdU+ cells). And at 14 days, control brains
214 averaged 1.5 EdU+ cells/brain (2 brains; 3 dividing cells) compared to 34.8 EdU+ cells/brain
215 following PTBI (8 brains; 278 EdU+ cells). Together these data demonstrate: 1) that glia can
216 divide to give rise to new glia; 2) that new neurons are created later than new glial cells; and 3)
217 that some of the Class I (EdU+) and/or Class IV (EdU+Repo+Elav+) cells may give rise to new
218 neurons (EdU+, Elav+). For reasons explained below, we favor the possibility that it is the
219 Class I cells that give rise to the new neurons.
220
221 <u>Expression of neural progenitor genes post-PTBI</u>
222 Although neural stem cells have been reported in the optic lobes of the adult Drosophila brain
223 (FERNANDEZ-HERNANDEZ *et al.* 2013), there are no known neural stem cells (neuroblasts) in the
224 adult Drosophila central brain. To test whether neuroblast fates were induced by injury and, if

225 so, whether the generation of new neurons followed a normal developmental trajectory, we
226 assayed the expression of multiple neural precursor genes post-PTBI using
227 immunohistochemistry and/or qRT-PCR. During normal Drosophila development, the central
228 brain neurons and glia derive from two types of neuroblasts (BOONE AND DOE 2008; EGGER *et*
229 *al.* 2008; WENG AND LEE 2011; HOMEM AND KNOBLICH 2012; HOMEM *et al.* 2015)2008. Type I
230 neuroblasts express the transcription factors Deadpan (Dpn) and Asense (Ase). Type II
231 neuroblasts express Dpn, but not Ase, and give rise to intermediate neural progenitors (INPs)
232 (BELLO *et al.* 2008; BOONE AND DOE 2008; BOWMAN *et al.* 2008). Immature INPs express the
233 transcription factor Ase, but not Dpn while mature INPs no longer express Ase, but reactivate
234 Dpn. Thus there is coexpression of Dpn and Ase in Type I, but not in Type II lineages. Other
235 transcription factors required during neurogenesis in the Type I and/or Type II lineages include
236 Inscuteable (Insc) and Earmuff (Erm) (CHIA *et al.* 2008).
237 In immunohistochemistry experiments, we probed control and injured brains from *ase-*
238 *Gal4, UAS-Stinger; UAS-Gal80^{ts}* adult males with anti-Dpn and anti-PH3 antibodies. These flies
239 were reared at 18°C where the temperature-sensitive Gal80 protein is functional and prevents
240 expression of green fluorescent protein (GFP) from the Stinger construct (BAROLO *et al.* 2000).
241 Within 6 hours of eclosion, adult male flies were subjected to PTBI and then placed at 30°C for
242 24 hours prior to dissection and immunostaining. At 30°C, the temperature-sensitive Gal80 is
243 not functional and GFP is expressed in *ase*-expressing cells. We observed clusters GFP+ cells
244 and cells that are PH3+Dpn+ in PTBI, but not control, brains (**Fig. 3A-D'''**). This indicates that
245 proliferating cells have a key feature of neuroblast identity, namely Dpn expression. We did not
246 observe cells that were PH3+Dpn+GFP+, i.e. dividing and coexpressing *dpn* and *ase*. However,
247 the juxtaposition of the PH3+Dpn+ cells to cells expressing *ase* is reminiscent of Type II
248 neuroblast lineages and consistent with the PH3+Dpn+ cells and Ase+ cells sharing a common
249 origin.

250 To quantify neural progenitor gene expression, we collected and injured young adult
251 males within 6 hours of eclosion. mRNA subsequently was extracted at 5 different time points (4
252 hours, 24 hours, 3 days, 7 days, and 14 days) from post-PTBI and age-matched, uninjured
253 control heads. Relative transcript levels of neural progenitor genes were measured using
254 quantitative real-time PCR (qRT-PCR). At 4 and 24 hours of age, *ase* expression is increased
255 greater than 2-fold in injured flies compared to controls (**Fig. 3E**). This difference diminishes by
256 3 days and is not significant at later timepoints (**Fig. 3E**). Although we observed Dpn+ cells
257 using immunohistochemistry near the area of injury at 24 hours post-PTBI, *dpn* mRNA levels
258 were not detectably increased at any timepoints (**Fig. 3F**). This could be because we isolated
259 RNA from whole heads and relatively few cells activate *dpn* following PTBI making it difficult to
260 detect an increase above baseline. Alternatively, the increase in Dpn protein levels could be due
261 to post-transcriptional events and not correspond to an increase in steady state mRNA levels.
262 Consistent with the idea that neural progenitor-like cell lineages are generated following PTBI,
263 *erm* transcript levels were increased at 4 hours and *insc* transcript levels were significantly
264 increased at 4 hours, 24 hours, and 3 days, while (**Fig. 3G, H**). *erm* is expressed in Type II
265 neuroblast lineages where it prevents reversion of intermediate neural progenitors to neuroblast
266 fates (WENG *et al.* 2010). *insc* is expressed in Type I neuroblast lineages where it prevents their
267 transformation into intermediate neural progenitors of the Type II lineage (AN *et al.* 2017).
268 Together these data support the hypothesis that there are neuroblast-like precursor cells in the
269 adult brain that are either induced or activated by PTBI.
270
271 <u>Lineage-tracing to identify the origins of newly created cells</u>
272 The presence of neuroblast-like cells post-PTBI could result from differentiated cells such as
273 glia or neurons dedifferentiating and adopting neuroblast-like fates; or via activation of a
274 quiescent population of adult neural stem cells, similar to what was described in the optic lobe
275 (FERNANDEZ-HERNANDEZ *et al.* 2013). To distinguish between these possibilities, we carried out

276 a series of lineage analyses. We first carried out lineage-tracing of glial cells and asked whether
277 they could become neurons. To do this, we used *repo-Gal4* in conjunction with a *flipout-GFP*
278 construct to permanently mark glial lineages. F1 males that were *w[*]; repo-*
279 *Gal4/P{w[+mC]=Ubi-p63E(FRT.STOP)Stinger}15F2* were injured at within 6 hours of eclosion
280 and aged for 14 days prior to dissection and immunostaining. We observed no *repo → GFP*
281 cells that were also Elav+ (not shown). This indicates that glia do not give rise to neurons
282 through either trans- or dedifferentiation. At first glance, these results appear inconsistent with
283 the observation of EdU+Repo+Elav+ cells shown in **Fig. 2D-D'''**. However, the cells with hybrid
284 glial-neuronal identity are quite small, and it was reported previously that neuroblasts that
285 undergo reducing divisions are destined for cell death (SIEGRIST *et al.* 2010). We therefore
286 postulate that the hybrid cells are inviable and do not contribute to the population of new
287 neurons (Class III cells) shown in **Fig. 2**. We note that ~50% of PH3+ and EdU+ cells post-PTBI
288 are glia (**Fig. 2F**). Thus, although we found no evidence that glia give rise to neurons, glia
289 nonetheless proliferate, especially early post-PTBI.
290 To test whether neurons can give rise to glia, we used a similar lineage-labeling
291 technique with an *Nsyb-Gal4* driver in a system called Gal4 technique for real-time and clonal
292 expression (G-TRACE) (EVANS *et al.* 2009). F1 males that were *w[*];Nsyb-*
293 *Gal4/P{w[+mC]=UAS-RedStinger}6,P{w[+mC]=UAS-FLP.Exel}3,P{w[+mC]=Ubi-*
294 *p63E(FRT.STOP)Stinger}15F* were injured within 6 hours of eclosion and aged for 14 days
295 prior to dissection and immunostaining. We observed no *NSyb → GFP* cells that were also
296 Repo+ (not shown). This indicates that neurons do not give rise to new glia post-injury.
297 To address the possibility that new neurons are created by a quiescent neuroblast-like
298 population, we used a similar lineage labeling technique, this time in combination with a
299 neuroblast driver, *dpn-Gal4*. To ensure that neuroblast cells were not labeled during
300 development, we added a temperature sensitive Gal80 and reared the crosses at 18°C. Under
301 these conditions, the Gal80 prevents transcriptional activation by Gal4, thus keeping the lineage

302 tracing system off. F1 males that were *w[*]; dpn-Gal4/P{w[+mC]=tubP-GAL80[ts]}20;*
303 *P{w[+mC]=UAS-RedStinger}6,P{w[+mC]=UAS-FLP.Exel}3,P{w[+mC]=Ubi-*
304 *p63E(FRT.STOP)Stinger}15F* were collected or injured within 6 hours of eclosion and aged for
305 14 days at 30°C prior to dissection and immunostaining. At 30°C, the temperature sensitive
306 Gal80 protein is inactivated and Gal4 can activate transcription. Indeed, 14 days post-injury, we
307 observed GFP+Elav+ cells in injured brains (arrowheads in **Fig. 4A-A'''**), but not in uninjured
308 age-matched controls (not shown). These results are consistent with the existence of a
309 quiescent stem cell-like population in the adult *Drosophila* brain that is activated by injury to
310 create new neurons. Several lines of evidence strongly support this view, including the presence
311 of Dpn+ and Ase+ cells near the area of injury 24 hours post-PTBI (**Figs. 3C-D'''**) and the
312 elevated expression levels *ase, erm,* and *insc* post-PTBI (**Fig. 3A-H**). However, because we do
313 not observe Dpn+ cells in our control uninjured central brains, these putative neuroblast-like
314 cells differ from the neuroblasts present during development in that they lack detectable *dpn*
315 expression until stimulated by PTBI.
316
317 Structural and Functional Regeneration post-PTBI
318 To visualize new neurons and their projections after PTBI, we utilized perma-twin labeling
319 (FERNANDEZ-HERNANDEZ *et al.* 2013). Perma-twin labeling permanently labels dividing cells and
320 their progeny with either green fluorescent protein (GFP) or red fluorescent protein (RFP). We
321 used adult F1 male flies of the genotype: *w; FRT40A, UAS-CD8-GFP, UAS- CD2-Mir/ FRT40A,*
322 *UAS-CD2-RFP, UAS-GFP-Mir; act-Gal4 UAS-flp/tub-Gal80^{ts}* that were reared at 17°C during
323 development to keep the labeling system switched off. Perma-twin flies were subjected to PTBI
324 within 24 hours of eclosion, and allowed to recover at 30°C for either 2, 7, or 14 days post-injury.
325 At 30°C, the labeling system is active and the progeny of any cells that divide may express
326 either GFP or RFP. As expected, based on our earlier finding that PTBI stimulates cell
327 proliferation, we observed more clones in injured samples than controls at all timepoints (**Fig.**

328 **5A-E**). We also found that injured brains had significantly more clones at later timepoints
329 compared to earlier ones, indicating that regeneration and proliferation were progressive and
330 were not limited to the time immediately after the initial injury (**Fig. 5A-E**). Interestingly, we
331 observed large clones at later timepoints that produced new MB neurons (**Fig. A-G**). These new
332 neurons project dendrites correctly to the MB calyx and axons correctly to the MB lobes. This
333 robust regeneration was observed in approximately 50% of the injured brains by 14 days post-
334 PTBI (**Fig. 5N**). Other areas of the brain also grew new neurons and new axon tracts. These
335 include the antennal lobes (AL), the ellipsoid body (EB), and the lateral horn (LH) (**Fig. 5H-M**) in
336 which we observed large clones approximately 26%, 26%, and 20% of the time, respectively
337 (**Fig. 5N**). These data suggest that there is structural repair of the damaged brains.
338 In order to assess functional recovery post-PTBI, we asked whether *Drosophila*
339 locomotor function is impaired by PTBI and, if so, whether function is restored at later
340 timepoints. 2-day post-PTBI flies, exhibited significantly different locomotor profiles from the
341 stereotypic locomotory patterns of age-matched controls (**Fig. 6A**). However, by 14 days post-
342 injury, by which time we also observed the generation of new neurons and axon tracts, the
343 injured flies displayed comparable locomotor profiles to age-matched controls (**Fig. 6B**). These
344 data indicate that PTBI significantly impacts motor function, and that this damage is largely
345 repaired by 14 days.
346
347 **Discussion**
348 Following a penetrating traumatic brain injury (PTBI), we find that the adult *Drosophila* central
349 brain has regenerative potential (**Fig. 7**). We demonstrate that PTBI rapidly stimulates cell
350 proliferation (**Fig. 1**) and that a robust proliferative response occurs primarily in young adult flies
351 and diminishes with age (**Figs. S1A and S1B**). Our data also indicate that age plays an
352 important role in the adult *Drosophila*'s ability to survive a traumatic injury (**Fig. S2B**), consistent
353 with the age-dependence of PTBI survival reported by Sanuki *et al.* (SANUKI *et al.* 2019). Within

354 one week of PTBI, both new glia and new neurons have been created (**Fig. 2**). At early
355 timepoints post-PTBI, but not in control brains, we observe dividing neuroblast-like cells that are
356 Dpn+ (**Fig. 3**). Other neural progenitor genes such as *ase*, *insc,* and *erm* exhibit elevated
357 transcript levels at early timepoints post-injury (**Fig. 3**). Using cell lineage-tracing techniques, we
358 found that new neurons are generated by cells that had expressed *dpn* (**Fig. 4**). These *dpn*-
359 expressing cells were not observed in uninjured controls. The newly created neurons contribute
360 to the overall regeneration of damaged brain tissue, particularly near the mushroom body (**Fig.**
361 **5**). The timing of regeneration corresponds with the timing of recovery of the locomotor activity
362 disrupted by PTBI (**Fig. 6**). This supports the idea that the newly generated neurons are both
363 functional and properly connected. However, we cannot rule out the possibility that other parts
364 of the brain are compensating for the damaged areas and that the behavioral improvement is
365 not a direct consequence of the new neurons.

366 We were intrigued to observe cells of hybrid glial (Repo+) and neuronal (Elav+) identity
367 in injured brains (**Fig. 2**), and initially thought these might represent a transitional state from glia
368 to neuron or from glia to neural precursor. Repo+Elav+ cells are not present in uninjured control
369 adult brains, but have been reported during larval development (BERGER *et al.* 2007) and in
370 certain brain tumors (BEAUCHER *et al.* 2007). Elav also is known to be transiently expressed in
371 some neuroblast-like cells during development (BEAUCHER *et al.* 2007). Thus, the presence of
372 dividing cells that are Repo+Elav+ is consistent with a less differentiated state. However, our
373 lineage studies do not support the hypothesis that these hybrid cells are the progenitors of
374 either glia or neurons. Specifically, while glia give rise to new glia, lineage tracing did not reveal
375 any new neurons derived from cells with prior glial identity, nor did it reveal any new glia derived
376 from cells with prior neuronal identity. Also notable is that the cells possessing the hybrid glial
377 and neuronal fate are quite small. Reducing divisions and small cell size previously were
378 correlated with apoptosis in Drosophila brains (SIEGRIST *et al.* 2010). Together, these results are

379 most consistent with the idea that cells possessing the hybrid glial and neuronal fate are
380 inviable.

381 Previous studies have indicated a higher occurrence of certain brain tumors, such as
382 glioblastomas, in people that have previously experienced TBI (TYAGI *et al.* 2016). However,
383 following PTBI, we do not find evidence of unregulated cell division. When young adult flies are
384 subjected to PTBI, there is a robust proliferative response that diminishes with time post-PTBI
385 (**Fig. S1A**). The proliferative response also diminishes with age and is negligible by 2 weeks
386 post-eclosion (**Fig. S1B**). By histology, we also do not see any evidence of tumor formation by
387 25 days post-PTBI (**Fig. S2E,G**). Neurodegeneration is another common consequence of brain
388 injury both in mammals (reviewed in (GRAHAM AND SHARP 2019)) and Drosophila
389 (KATZENBERGER *et al.* 2013) and is thought to result from secondary brain injury, i.e. from
390 cascades triggered by trauma and not the trauma itself (reviewed in (NG AND LEE 2019)). We do
391 observe limited neurodegeneration following PTBI (**Fig. S2E,G**). This is consistent with a small
392 amount of cell death in the first hours after PTBI (**Fig. S2C-D', F**). However, cell death is
393 restricted by 24 hours post-PTBI and indistinguishable from controls by 10 days post-PTBI (**Fig.**
394 **S2F**). This limited cell death and neurodegeneration may contribute to a small reduction in
395 lifespan observed post-PTBI (**Fig. S1A**). Together, our results support the ideas that secondary
396 injury is minimal in our PTBI model and that PTBI does not stimulate uncontrolled cell division.
397 The mechanisms underlying what appears to be a tightly-regulated process need to be further
398 analyzed to understand how *Drosophila* are able to give a measured proliferative cell response
399 to regenerate damaged tissue.

400 We detect both new glia and new neurons post-PTBI, but these cell types are not
401 generated in equal proportions or on the same time scale. There is an initial wave of
402 gliogenesis, followed by a delayed wave of neurogenesis (**Fig. 2**). Glial proliferation is a known
403 response to neuronal injury in both mammals and Drosophila, with the added glia participating

404 in phagocytosis of cellular debris (reviewed in (BURDA AND SOFRONIEW 2014; PEKNY AND PEKNA
405 2016)). The newly-generated glia may play similar roles following PTBI.
406 In addition to proliferating glial cells, we have identified a distinct population of cells that
407 divide to give rise to new neurons. These cells do not express either Repo nor Elav, i.e. they are
408 neither glia nor neurons. In addition, although our lineage analysis indicates that the new
409 neurons arise from cells that express *dpn* (**Fig. 4**), we do not detect *dpn* expression in uninjured
410 adult central brains with either Dpn antibodies or *dpn* reporters. We therefore propose that *dpn*
411 expression is activated by central brain injury, and that cells that activate *dpn* expression give
412 rise to new neurons. *dpn* encodes a basic helix-loop-helix (bHLH) transcriptional repressor
413 orthologous to mammalian HES1 (BIER *et al.* 1992; YOUNGER-SHEPHERD *et al.* 1992). During
414 normal Drosophila neural development Dpn represses the expression of neural differentiation
415 genes (KANG AND REICHERT 2015; RAMON-CANELLAS *et al.* 2019; LI AND HIDALGO 2020). Thus,
416 the upregulation of *dpn* expression post-PTBI may confer neural progenitor fate on these cells
417 and be an essential step in adult neurogenesis. Our data support the idea that there is a
418 quiescent population of cells in uninjured brains that cannot be detected with standard neuronal,
419 glial, or neuroblast markers, but that nonetheless has regenerative potential. If such cells exist
420 in *Drosophila*, perhaps they also exist in humans. An important avenue for future research
421 includes the generation of gene expression profiles and markers for these progenitor cells such
422 that they can be visualized in and sorted from uninjured brains in order to explore the
423 mechanisms of their activation.
424 We note that in the optic lobe, cells with cytoplasmic Dpn protein were identified and
425 proposed to be quiescent neural progenitors, with nuclear translocation of Dpn following injury
426 correlated with adult neurogenesis (FERNANDEZ-HERNANDEZ *et al.* 2013). We do not observe
427 either nuclear or cytoplasmic Dpn protein in the uninjured central brain. Nor have we observed
428 GFP expression driven by the *dpn-GAL4* reporter in the uninjured central brain. Thus, while
429 there is a quiescent neural progenitor cells identifiable with standard markers in the optic lobe,

430 this does not appear to be the case in the central brain. A second difference between adult
431 neurogenesis in the optic lobe and the central brain involves expression of the neural progenitor
432 gene *ase*. In the optic lobe, *ase* is not upregulated by injury (FERNANDEZ-HERNANDEZ *et al.*
433 2013). In contrast, in the central brain after PTBI, there is *ase* upregulation as assayed by both
434 qRT-PCR and immunohistochemistry (**Fig. 3**). Interestingly, the *ase*-expressing cells are in
435 close proximity to *dpn*-expressing cells (**Fig. 3**). This is reminiscent of normal neural
436 development in Type II neuroblast lineages (BELLO *et al.* 2008; BOONE AND DOE 2008; BOWMAN
437 *et al.* 2008). Nonetheless, the expression of both Type I (*insc*) and Type II (*erm*) lineage
438 attributes suggests that these cells do not recapitulate larval neurogenesis. A third difference
439 between adult neurogenesis in the optic lobe and the central brain is that optic lobe injury does
440 not result in the generation of new glia. In contrast, glial proliferation is rapid and robust
441 following central brain injury (**Fig. 2**). Together, these results indicate that adult central brain
442 neurogenesis differs from adult neurogenesis in the optic lobe. Given that the neural
443 progenitors of the optic lobes and central brain follow distinct developmental trajectories
444 (RAMON-CANELLAS *et al.* 2019), it perhaps should not come as a surprise that their regenerative
445 capacities and programs also are different.
446 Using a PTBI paradigm, we have been able to establish that young adult *Drosophila* are
447 capable of robust regeneration, with the creation of new neurons and glia and functional
448 recovery from locomotor defects by 14 days post-PTBI. Further questions remain about the
449 origin and properties of the neural progenitor cells and the molecular mechanisms that trigger
450 regeneration. Nonetheless, because brain regeneration can be stimulated by mild injury in adult
451 Drosophila, there is an avenue by which to identify these cells and mechanisms for future study.
452 In addition, the Drosophila adult central brain now provides a novel model system for screening
453 pharmacologic agents for those that activate the regenerative program. This could lead to new
454 therapeutic approaches for both neurodegenerative diseases and brain injuries.
455

456 **Materials & Methods**

457 Fly Stocks and Rearing

458 Unless otherwise specified, flies were reared at 25°C on a standard cornmeal-sugar medium.
459 The following stocks were obtained from the Bloomington Drosophila Stock Center (BDSC):
460 **#854** (*w[*]; P{w[+mW.hs]=GawB}OK107 ey[OK107]/In(4)ci[D], ci[D] pan[ciD] sv[spa-pol]*; **#1495**
461 (*y[1] w[1]*); **#4539** *y[1] w[*]; P{w[+mC]=UAS-FLP.D}JD1*; **#5130** (*y[1] w[1]; Pin[Yt]/CyO;*
462 *P{w[+mC]=UAS-mCD8::GFP.L}LL6)*; **#7018** (*w[*]; sna[Sco]/CyO;P{w[+mC]=tubP-*
463 *GAL80[ts]}ncd[GAL80ts-7]*); **#7019** (*w[*];P{w[+mC]=tubP-GAL80[ts]}20;TM2/TM6B, Tb[1]*;
464 **#7415** (*w^{1118}; P{w[+m*]=GAL4}repo/TM3, Sb^1*); **#28281** (*w[*];P{w[+mC]=UAS-*
465 *RedStinger}6,P{w[+mC]=UAS-FLP.Exel}3,P{w[+mC]=Ubi-p63E(FRT.STOP)Stinger}15F*);
466 **#32251** (*w[*]; P{w[+mC]=Ubi-p63E(FRT.STOP)Stinger}15F2*); **#47859** *w[1118]; P{y[+t7.7]*
467 *w[+mC]=GMR13CO2-GAL4}attP2*; **#51635** (*y^1 w^*; P{w[+m*]=nSyb-GAL4S}3*): **#65408**
468 (*P{w[+mC]=UAS-Stinger}2, P{w[+mC]=UAS-hid.Z}2/CyO*). Other lines used were *ase-*
469 *Gal4/CyO; Dr/TM6B* (a gift of Dr. Cheng-Yu Lee); *w; FRT40A, UAS-CD8-GFP, UAS- CD2-Mir;*
470 *act-Gal4 UAS-flp/TM6B*; and *w; FRT40A, UAS-CD2-RFP, UAS-GFP-Mir; tub-Gal80ts/TM6B*
471 (both gifts of Dr. Eduardo Moreno).
472

473 Standard cross

474 To minimize potentially confounding genetic background effects and differences in results due
475 to sex and temperature, we routinely analyzed F1 males of a standard genotype. This standard
476 genotype results from an outcross between a homozygous strain expressing green fluorescent
477 protein (GFP) in the mushroom body (*w*; UAS-mCD8-GFP;; OK107-Gal4*) and the widely used
478 laboratory strain *y^1 w^1*. This cross was maintained at 25°C. PTBI flies were kept at 25°C until
479 their brains were dissected and fixed for analysis. Unless otherwise specified, brains of young
480 adult male *Drosophila* generated by this outcross were injured within 6 hours of eclosion.
481

482 Perma-twin flies

483 Perma-twin flies were generated by crossing *w; FRT40A, UAS-CD2-RFP, UAS-GFP-Mir; tub-*
484 *Gal80^{ts}/TM6B* virgin females to *w; FRT40A, UAS-CD8-GFP, UAS- CD2-Mir; act-Gal4 UAS-*
485 *flp/TM6B* males (FERNANDEZ-HERNANDEZ *et al.* 2013). These crosses were maintained at 17°C.
486 F1 progeny of the genotype: *w; FRT40A, UAS-CD8-GFP, UAS- CD2-Mir/ FRT40A, UAS-CD2-*
487 *RFP, UAS-GFP-Mir; act-Gal4 UAS-flp/tub-Gal80^{ts}* were collected at eclosion, subjected to PTBI
488 or kept as uninjured controls and maintained at 30°C until their brains were dissected and fixed
489 for analysis.

490

491 G-TRACE crosses

492 Lineage-labeling was accomplished using a G-TRACE line (**#28281** (*w[*];P{w[+mC]=UAS-*
493 *RedStinger}6,P{w[+mC]=UAS-FLP.Exel}3,P{w[+mC]=Ubi-p63E(FRT.STOP)Stinger}15F*)
494 (EVANS *et al.* 2009) crossed to various Gal4 driver strains listed above. These crosses were
495 maintained at 17°C. F1 progeny of the desired genotyped were selected at eclosion, subjected
496 to PTBI or kept as uninjured controls and maintained at 30°C for 14 days when their brains were
497 dissected and fixed for analysis.

498

499 Penetrating Traumatic Brain Injury

500 To induce PTBI, we used thin metal needles (~12.5 μm diameter tip, 100 μm diameter rod; Fine
501 Science Tools) sterilized in 70% ethanol to penetrate the head capsule of CO_2-anesthetized
502 adult flies. Injured flies were transferred back to our standard sugar food for recovery and aging.
503 For immunohistochemical analyses, we unilaterally injured brains on their right sides. For qRT-
504 PCR analysis, to amplify the molecular responses, brains were injured bilaterally.

505

506

507

508 Immunohistochemistry

509 Brains were dissected in PBS (phosphate-buffered saline; 100 mM K_2HPO4, 140 mM NaCl pH
510 7.0) and fixed in a 3.7% formaldehyde in a PEM (100 mM PIPES, 2 mM EGTA, 1 mM $MgSO_4$)
511 solution for 20 minutes at 25°C. Fixed brain samples were washed in PT (PBS and 0.1% Triton
512 X-100), blocked with 2% BSA in PT solution (PBT), and then incubated with primary antibodies
513 overnight at 4°C in PBT. Following primary antibody incubation, the samples were washed with
514 PT (5 times over the course of an hour) and incubated overnight in secondary antibody at 4°C.
515 The next day, samples were washed in PT, stained with DAPI (1:10,000, ThermoFisher) for 8
516 minutes, and mounted in Vectashield anti-fade mountant (Vector Labs) and imaged using a
517 Nikon A1RS system and analyzed using the Nikon NIS Elements software. Cell counting was
518 done both manually and using the Nikon NIS-Elements software to analyze regions of interest
519 (ROIs) with a threshold of over 1000 and an area of at least 10μm.

520 The primary antibodies used in this study were: rabbit anti-PH3 (1:500, Santa Cruz
521 Biotechnology, Inc); mouse anti-FasII (1:20, Developmental Studies Hybridoma Bank; DSHB);
522 mouse anti-Repo (1:20, DSHB); rat anti-Elav (1:20, DSHB); mouse anti-Pros (1:20, DSHB); and
523 rat anti-Dpn (1:50, AbCam). Secondary antibodies used were: anti-rabbit Alexa Fluor 568
524 (1:200, ThermoFisher); anti-rabbit Cy5 (1:400, Jackson ImmunoResearch, Inc.); anti-mouse
525 Cy5 (1:100, Jackson ImmunoResearch, Inc.); anti-rat Alexa Fluor 488 (1:400, ThermoFisher);
526 anti-rat Alexa Fluor 568 (1:400, ThermoFisher); and anti-rat Cy5 (1:200, Jackson
527 ImmunoResearch, Inc.).

528

529 EdU labeling

530 The standard injury method was used on flies for 5-ethynyl-2'-deoxyuridine (EdU) labeling,
531 except flies were fed 50 mM EdU in 10% sucrose solution on a size 3 Whatman filter for six
532 hours prior to PTBI and allowed to recover on the same solution for the desired amount of time.
533 The EdU solution was replaced every 24 hours. Brains were dissected, processed, and antibody

534 stained as described above with the exception of using buffers without azide. To detect EdU
535 incorporation, Click-IT® reagents from InVitrogen were used according to the manufacturer's
536 instructions. The brains then were antibody stained mounted and imaged as described above.
537
538 Quantitative Real-Time PCR
539 Transcript levels of target genes were measured by quantitative real-time PCR (qRT-PCR)
540 using methods described in (IHRY *et al.* 2012). RNA was isolated from appropriately staged
541 animals using TRIzol Reagent used according to the manufacturer's instructions (Thermo Fisher
542 Scientific). cDNA was synthesized from 40 to 400 ng of total RNA using the SuperScript III First-
543 Strand Synthesis System (Invitrogen). qPCR was performed on a Roche 480 LightCycler using
544 the LightCycler 480 DNA SYBR Green I Master kit (Roche). In all cases, samples were run
545 simultaneously with three independent biological replicates for each target gene, and *rp49* was
546 used as the reference gene. To calculate changes in relative expression, the Relative
547 Expression Software Tool was used (PFAFFL *et al.* 2002). We used the following primers to
548 detect transcript levels: *ase* Forward: 5'-CAGTGATCTCCTGCCTAGTTTG-3' & Reverse: 5'-
549 GTGTTGGTTCCTGGTATTCTGATG-3' (gift from Stanislava Chtarbanova); *dpn* Forward: 5'-
550 CGCTATGTAAGCCAAATGGATGG-3' & Reverse: 5'-CTATTGGCACACTGGTTAAGATGG-3'
551 (gift from Stanislava Chtarbanova); *elav* Forward: 5'-CGCAGCCCAATACGAATGG-3' &
552 Reverse: 5'-CATTGTTTGCGGCAA GTAGTTG-3' (Fly Primer Bank; (HU *et al.* 2013)); *erm*
553 Forward: 5'- GTCCCCTAAAGTTTTCGATAGCC-3' & Reverse: 5'-
554 GAGTCATAGTTGACAGTGGATGG-3' (Fly Primer Bank); *insc* Forward: 5'-
555 CCCTGGGCAATCTGTCCTG-3' & Reverse: 5'- GAGAAGCCCGAATCCTGACT-3' (Fly Primer
556 Bank); *myc* Forward: 5'- AGCCAGAGATCCGCAACATC-3' & Reverse: 5'-
557 CGCGCTGTAGAGATTCGTAGAG-3' (Fly Primer Bank); *repo* Forward: 5'-
558 TCGCCCAACTATGTGACCAAG-3' & Reverse: 5'-CGGCGCACTAATGTACTCG-3' (Fly Primer

559 Bank;; *Rp49* Forward: 5'-CCAGTCGGATCGATATGCTAA-3' & Reverse: 5'-
560 ACGTTGTGCACCAGGAACTT-3' (IHRY *et al.* 2012).
561
562 Locomotor assays
563 0-6-hour post-eclosion *OK107/yw* males were collected, subjected to PTBI, and aged to 2 days
564 and 14 days, respectively. The 2 and 14 day injured and age-matched uninjured controls were
565 placed in the *Drosophila* Activity Monitor (DAM) system (TriKinetics, Waltham, MA) to record
566 locomotory behavior. The circadian locomotor activity of flies was assayed and analyzed as
567 previously described (HAMBLEN *et al.* 1986; SEHGAL *et al.* 1992). For each experiment and
568 condition, 32 flies were individually analyzed.
569
570 Statistical analysis
571 For all cell/clone counting and locomotor assays, counts were expressed as means ± standard
572 deviations. Two-tailed t-tests were performed using GraphPad Prism Version 8.3.0 for Mac
573 (GraphPad Software, La Jolla California USA, www.graphpad.com). An alpha value of 0.05 was
574 considered significant. The following symbols represent significance; * significant at $p \leq 0.05$; **
575 significant at $p \leq 0.01$; *** significant at $p \leq 0.001$; **** significant at $p \leq 0.0001$.
576
577 Reagent sharing statement
578 Strains are available upon request. The authors affirm that all data necessary for confirming the
579 conclusions of the article are present within the article, figures, and tables.
580
581 **Acknowledgements**
582 We are grateful to Becky Katzenberger and Sarah Neuman for technical assistance; Eduardo
583 Moreno for sharing the Perma-twin stocks; and Stanislava Chtarbanova for the *ase* and *dpn*
584 primers. We also would like to thank Barry Ganetzky and David Wassarman for lively

585 discussions that undoubtedly improved the science and Kent Mok, Cayla Guerra, Bailey
586 Spiegelberg, and Shawn Ahern-Djamali for their contributions to the laboratory. The FasII, Elav
587 and Repo monoclonal antibodies were obtained from the Developmental Studies Hybridoma
588 Bank, created by the NICHD of the NIH and maintained at The University of Iowa, Department
589 of Biology, Iowa City, IA 52242. Most of the Drosophila strains used in this study were obtained
590 from the Bloomington Drosophila Stock Center (BDSC; NIH P40OD018537). This work was
591 supported by NIH T32 GM007133 (KLC and KM); NIH NS090190 (GBF); NIH NS102698 (GBF);
592 the University of Wisconsin Graduate School (GBF); and the Women in Science and
593 Engineering Leadership Institute (WISELI) (GBF).
594

595 **References cited**

596 Altman, J., 1969 Autoradiographic and histological studies of postnatal neurogenesis. IV. Cell
597 proliferation and migration in the anterior forebrain, with special reference to persisting
598 neurogenesis in the olfactory bulb. J Comp Neurol 137**:** 433-457.
599 Altman, J., and G. D. Das, 1965 Autoradiographic and histological evidence of postnatal
600 hippocampal neurogenesis in rats. J Comp Neurol 124**:** 319-335.
601 Amariglio, N., A. Hirshberg, B. W. Scheithauer, Y. Cohen, R. Loewenthal *et al.*, 2009 Donor-
602 derived brain tumor following neural stem cell transplantation in an ataxia telangiectasia
603 patient. PLoS Med 6**:** e1000029.
604 An, H., W. Ge, Y. Xi and X. Yang, 2017 Inscuteable maintains type I neuroblast lineage identity
605 via Numb/Notch signaling in the Drosophila larval brain. J Genet Genomics 44**:** 151-162.
606 Aso, Y., D. Hattori, Y. Yu, R. M. Johnston, N. A. Iyer *et al.*, 2014 The neuronal architecture of
607 the mushroom body provides a logic for associative learning. Elife 3**:** e04577.
608 Barolo, S., L. A. Carver and J. W. Posakony, 2000 GFP and beta-galactosidase transformation
609 vectors for promoter/enhancer analysis in Drosophila. Biotechniques 29**:** 726, 728, 730,
610 732.
611 Beaucher, M., J. Goodliffe, E. Hersperger, S. Trunova, H. Frydman *et al.*, 2007 Drosophila brain
612 tumor metastases express both neuronal and glial cell type markers. Dev Biol 301**:** 287-
613 297.
614 Bellen, H. J., C. Tong and H. Tsuda, 2010 100 years of Drosophila research and its impact on
615 vertebrate neuroscience: a history lesson for the future. Nat Rev Neurosci 11**:** 514-522.
616 Bello, B. C., N. Izergina, E. Caussinus and H. Reichert, 2008 Amplification of neural stem cell
617 proliferation by intermediate progenitor cells in Drosophila brain development. Neural
618 Dev 3**:** 5.
619 Berger, C., S. Renner, K. Luer and G. M. Technau, 2007 The commonly used marker ELAV is
620 transiently expressed in neuroblasts and glial cells in the Drosophila embryonic CNS.
621 Dev Dyn 236**:** 3562-3568.
622 Bier, E., H. Vaessin, S. Younger-Shepherd, L. Y. Jan and Y. N. Jan, 1992 deadpan, an
623 essential pan-neural gene in Drosophila, encodes a helix-loop-helix protein similar to the
624 hairy gene product. Genes Dev 6**:** 2137-2151.
625 Boone, J. Q., and C. Q. Doe, 2008 Identification of Drosophila type II neuroblast lineages
626 containing transit amplifying ganglion mother cells. Dev Neurobiol 68**:** 1185-1195.
627 Bowman, S. K., V. Rolland, J. Betschinger, K. A. Kinsey, G. Emery *et al.*, 2008 The tumor
628 suppressors Brat and Numb regulate transit-amplifying neuroblast lineages in
629 Drosophila. Dev Cell 14**:** 535-546.
630 Burda, J. E., and M. V. Sofroniew, 2014 Reactive gliosis and the multicellular response to CNS
631 damage and disease. Neuron 81**:** 229-248.
632 Cao, Y., S. Chtarbanova, A. J. Petersen and B. Ganetzky, 2013 Dnr1 mutations cause
633 neurodegeneration in Drosophila by activating the innate immune response in the brain.
634 Proc Natl Acad Sci U S A 110**:** E1752-1760.
635 Chia, W., W. G. Somers and H. Wang, 2008 Drosophila neuroblast asymmetric divisions: cell
636 cycle regulators, asymmetric protein localization, and tumorigenesis. J Cell Biol 180**:**
637 267-272.
638 Dewan, M. C., A. Rattani, S. Gupta, R. E. Baticulon, Y. C. Hung *et al.*, 2018 Estimating the
639 global incidence of traumatic brain injury. J Neurosurg**:** 1-18.
640 Egger, B., J. M. Chell and A. H. Brand, 2008 Insights into neural stem cell biology from flies.
641 Philos Trans R Soc Lond B Biol Sci 363**:** 39-56.
642 Eriksson, P. S., E. Perfilieva, T. Bjork-Eriksson, A. M. Alborn, C. Nordborg *et al.*, 1998
643 Neurogenesis in the adult human hippocampus. Nat Med 4**:** 1313-1317.

644 Erkkinen, M. G., M. O. Kim and M. D. Geschwind, 2018 Clinical Neurology and Epidemiology of
645 the Major Neurodegenerative Diseases. Cold Spring Harb Perspect Biol 10.
646 Evans, C. J., J. M. Olson, K. T. Ngo, E. Kim, N. E. Lee *et al.*, 2009 G-TRACE: rapid Gal4-based
647 cell lineage analysis in Drosophila. Nat Methods 6**:** 603-605.
648 Fernandez-Hernandez, I., C. Rhiner and E. Moreno, 2013 Adult neurogenesis in Drosophila.
649 Cell Rep 3**:** 1857-1865.
650 Gao, X., X. Wang, W. Xiong and J. Chen, 2016 In vivo reprogramming reactive glia into iPSCs
651 to produce new neurons in the cortex following traumatic brain injury. Sci Rep 6**:** 22490.
652 Graham, N. S., and D. J. Sharp, 2019 Understanding neurodegeneration after traumatic brain
653 injury: from mechanisms to clinical trials in dementia. J Neurol Neurosurg Psychiatry 90**:**
654 1221-1233.
655 Grasl-Kraupp, B., B. Ruttkay-Nedecky, H. Koudelka, K. Bukowska, W. Bursch *et al.*, 1995 In situ
656 detection of fragmented DNA (TUNEL assay) fails to discriminate among apoptosis,
657 necrosis, and autolytic cell death: a cautionary note. Hepatology 21**:** 1465-1468.
658 Hamblen, M., W. A. Zehring, C. P. Kyriacou, P. Reddy, Q. Yu *et al.*, 1986 Germ-line
659 transformation involving DNA from the period locus in Drosophila melanogaster:
660 overlapping genomic fragments that restore circadian and ultradian rhythmicity to per0
661 and per- mutants. J Neurogenet 3**:** 249-291.
662 Hans, F., and S. Dimitrov, 2001 Histone H3 phosphorylation and cell division. Oncogene 20**:**
663 3021-3027.
664 Homem, C. C., and J. A. Knoblich, 2012 Drosophila neuroblasts: a model for stem cell biology.
665 Development 139**:** 4297-4310.
666 Homem, C. C., M. Repic and J. A. Knoblich, 2015 Proliferation control in neural stem and
667 progenitor cells. Nat Rev Neurosci 16**:** 647-659.
668 Hu, Y., R. Sopko, M. Foos, C. Kelley, I. Flockhart *et al.*, 2013 FlyPrimerBank: an online
669 database for Drosophila melanogaster gene expression analysis and knockdown
670 evaluation of RNAi reagents. G3 (Bethesda) 3**:** 1607-1616.
671 Ihry, R. J., A. L. Sapiro and A. Bashirullah, 2012 Translational control by the DEAD Box RNA
672 helicase belle regulates ecdysone-triggered transcriptional cascades. PLoS Genet 8**:**
673 e1003085.
674 Ito, K., W. Awano, K. Suzuki, Y. Hiromi and D. Yamamoto, 1997 The Drosophila mushroom
675 body is a quadruple structure of clonal units each of which contains a virtually identical
676 set of neurones and glial cells. Development 124**:** 761-771.
677 Ito, K., and Y. Hotta, 1992 Proliferation pattern of postembryonic neuroblasts in the brain of
678 Drosophila melanogaster. Dev Biol 149**:** 134-148.
679 Kang, K. H., and H. Reichert, 2015 Control of neural stem cell self-renewal and differentiation in
680 Drosophila. Cell Tissue Res 359**:** 33-45.
681 Kaplan, M. S., and J. W. Hinds, 1977 Neurogenesis in the adult rat: electron microscopic
682 analysis of light radioautographs. Science 197**:** 1092-1094.
683 Katzenberger, R. J., C. A. Loewen, D. R. Wassarman, A. J. Petersen, B. Ganetzky *et al.*, 2013
684 A Drosophila model of closed head traumatic brain injury. Proc Natl Acad Sci U S A 110**:**
685 E4152-4159.
686 Kuhn, H. G., H. Dickinson-Anson and F. H. Gage, 1996 Neurogenesis in the dentate gyrus of
687 the adult rat: age-related decrease of neuronal progenitor proliferation. J Neurosci 16**:**
688 2027-2033.
689 Lessing, D., and N. M. Bonini, 2009 Maintaining the brain: insight into human
690 neurodegeneration from Drosophila melanogaster mutants. Nat Rev Genet 10**:** 359-370.
691 Li, G., and A. Hidalgo, 2020 Adult Neurogenesis in the Drosophila Brain: The Evidence and the
692 Void. Int J Mol Sci 21.
693 Moreno, E., Y. Fernandez-Marrero, P. Meyer and C. Rhiner, 2015 Brain regeneration in
694 Drosophila involves comparison of neuronal fitness. Curr Biol 25**:** 955-963.

695 Ng, S. Y., and A. Y. W. Lee, 2019 Traumatic Brain Injuries: Pathophysiology and Potential
696 Therapeutic Targets. Front Cell Neurosci 13**:** 528.
697 Pekny, M., and M. Pekna, 2016 Reactive gliosis in the pathogenesis of CNS diseases. Biochim
698 Biophys Acta 1862**:** 483-491.
699 Pfaffl, M. W., G. W. Horgan and L. Dempfle, 2002 Relative expression software tool (REST) for
700 group-wise comparison and statistical analysis of relative expression results in real-time
701 PCR. Nucleic Acids Res 30**:** e36.
702 Ramon y Cajal, S., 1913 *Estudios sobre la degeneracio´n y regeneracio´n del sistema nervioso.*
703 *Tomo I, Degeneracio´n y regeneracio´n de los nervios.* Imprenta de Hijos de Nicola`s
704 Moya, Madrid.
705 Ramon y Cajal, S., 1914 *Estudios sobre la degeneracio`n y regeneracio´n del sistema nervioso*
706 *Tomo II, Degeneracio¨n y regeneracio´n de los centros nerviosos.* Imprenta de Hijos de
707 Nicola`s Moya, Madrid.
708 Ramon-Canellas, P., H. P. Peterson and J. Morante, 2019 From Early to Late Neurogenesis:
709 Neural Progenitors and the Glial Niche from a Fly's Point of View. Neuroscience 399**:** 39-
710 52.
711 Rimkus, S. A., R. J. Katzenberger, A. T. Trinh, G. E. Dodson, R. S. Tibbetts *et al.*, 2008
712 Mutations in String/CDC25 inhibit cell cycle re-entry and neurodegeneration in a
713 Drosophila model of Ataxia telangiectasia. Genes Dev 22**:** 1205-1220.
714 Sanuki, R., T. Tanaka, F. Suzuki, K. Ibaraki and T. Takano, 2019 Normal aging hyperactivates
715 innate immunity and reduces the medical efficacy of minocycline in brain injury. Brain
716 Behav Immun 80**:** 427-438.
717 Sehgal, A., J. Price and M. W. Young, 1992 Ontogeny of a biological clock in Drosophila
718 melanogaster. Proc Natl Acad Sci U S A 89**:** 1423-1427.
719 Siegrist, S. E., N. S. Haque, C. H. Chen, B. A. Hay and I. K. Hariharan, 2010 Inactivation of both
720 Foxo and reaper promotes long-term adult neurogenesis in Drosophila. Curr Biol 20**:**
721 643-648.
722 Tyagi, V., J. Theobald, J. Barger, M. Bustoros, N. S. Bayin *et al.*, 2016 Traumatic brain injury
723 and subsequent glioblastoma development: Review of the literature and case reports.
724 Surg Neurol Int 7**:** 78.
725 Vishwakarma, S. K., A. Bardia, S. K. Tiwari, S. A. Paspala and A. A. Khan, 2014 Current
726 concept in neural regeneration research: NSCs isolation, characterization and
727 transplantation in various neurodegenerative diseases and stroke: A review. J Adv Res
728 5**:** 277-294.
729 von Trotha, J. W., B. Egger and A. H. Brand, 2009 Cell proliferation in the Drosophila adult brain
730 revealed by clonal analysis and bromodeoxyuridine labelling. Neural Dev 4**:** 9.
731 Weng, M., K. L. Golden and C. Y. Lee, 2010 dFezf/Earmuff maintains the restricted
732 developmental potential of intermediate neural progenitors in Drosophila. Dev Cell 18**:**
733 126-135.
734 Weng, M., and C. Y. Lee, 2011 Keeping neural progenitor cells on a short leash during
735 Drosophila neurogenesis. Curr Opin Neurobiol 21**:** 36-42.
736 Younger-Shepherd, S., H. Vaessin, E. Bier, L. Y. Jan and Y. N. Jan, 1992 deadpan, an
737 essential pan-neural gene encoding an HLH protein, acts as a denominator in
738 Drosophila sex determination. Cell 70**:** 911-922.
739 Zhou, C., B. E. Grottkau and S. Zou, 2016 Regulators of Stem Cells Proliferation in Tissue
740 Regeneration. Curr Stem Cell Res Ther 11**:** 177-187.
741

742

743 **Figure Legends**

744 **Figure 1. Penetrating Traumatic Brain Injury (PTBI) stimulates cell proliferation. A.**
745 Schematic of an adult Drosophila head with the injury trajectory indicated in grey. Central brain
746 PTBI impacts multiple brain structures including the mushroom body (MB, green), and tissues
747 outside the brain including the fat body (blue) and hemocytes (red). CB = central brain region.
748 OL= optic lobe region. Uninjured, control (**B**) and PTBI **(C)** schematics. The blue boxes in the
749 upper right corners indicate the brain regions shown at higher magnification in panels **D-I. D**, **E**.
750 PH3 antibody (red) was used to assay for cell proliferation 24 hours after injury. In control brains
751 (**D)** there are few PH3+ cells, and none near the MB. However, in PTBI brains (**E**), there are PH3+
752 cells near the MB. **F, G.** To test whether newly created cells are surviving or being eliminated, we
753 conducted a pulse-chase EdU experiment. Flies were fed EdU (red) for 4 days post-injury (a
754 pulse) then chased for 3 days without feeding EdU. In the control brain (**F**), there is little EdU
755 incorporation. In the PTBI brain (**G**), there are EdU+ cells near the MB. **H.** In 14-day control brains,
756 there are few EdU+ cells. **I.** However, in 14-day PTBI brains, there is an increase in EdU+ cells
757 near the MB. All brains are from males of our standard genotype. **J.** Quantification of proliferating
758 cells. At 24 hours, uninjured control brains had an average of 3 PH3+ cells/brain (n=11 brains, 28
759 cells), while 24-hour post-PTBI brains had an average of 11 PH3+ cells/brain (n=17 brains, 181
760 cells). At 7 days, uninjured controls have few EdU+ cells, with an average of 2 EdU+ cells/brain
761 (n=15 brains, 24 cells), while 7-day post-PTBI brains had an average of 11 EdU+ cells/brain (n=22
762 brains, 238 cells). At 14 days, uninjured controls have an average of 1 EdU+ cell/brain (n=8
763 brains,11 cells), while 14-day post-PTBI brains have an average of 29 EdU+ cells/brain (n=14
764 brains, 400 cells). Unpaired t tests of control and PTBI samples at the 3 time points yield values
765 of $p<0.0001$, $p<0.0001$ and $p<0.0002$, respectively. Error bars reflect the standard deviation (SD).
766

767 **Figure 2. Analysis of new cell identities 7 days post-PTBI.** To determine what types of new
768 cells are generated in the first 7 days post-PTBI, we used pulse-chase experiments with EdU in

769 combination with the glial marker anti-Repo and the neuronal marker anti-Elav. At 7 days post-
770 PTBI, we found four classes of cells resulting from proliferation: EdU+ and without either Repo
771 or Elav (**A-A'''**; Class I); Cells that were EdU+ and Repo+ (**B-B'''**; Class II); EdU+ and Elav+ (**C-**
772 **C'''**; Class III); and EdU+, Repo+, Elav+ (**D-D'''**; Class IV). Arrowheads indicate representative
773 cells in each class. The nuclear dye DAPI is in blue. We then measured the changing ratios of
774 these cell types over time in control (**E**) and PTBI brains (**F**). For controls, 11 brains and 28 PH3+
775 cells were analyzed at 24 hours, 9 brains and 15 EdU+ cells were analyzed at 7 days, and 2
776 brains and 3 EdU+ cells were analyzed at 14 days. For PTBI samples, 17 brains and 181 PH3+
777 cells were analyzed at 24 hours, 15 brains and 172 EdU+ cells were analyzed at 7 days, and 8
778 brains and 278 EdU+ cells were analyzed at 14 days.
779
780 **Figure 3. Neuroblast gene expression is activated by PTBI. (A)** and (**C**) are low magnification
781 views of the control and PTBI brains shown at higher resolution in **B-B'''** and **D-D'''**, respectively.
782 **A-B'''.** Images from an uninjured *ase-Gal4, UAS-Stinger; UAS-Gal80^{ts}* probed with anti-PH3 (red)
783 and anti-Dpn (cyan). GFP (green) from the *UAS-Stinger* construct is expressed under control of
784 *ase* regulatory sequences. The nuclear dye DAPI is in blue. Arrowheads in (**A**) and (**C**) indicate
785 the regions where higher magnification images were collected. Animals were reared at 18°C
786 where the temperature-sensitive Gal80 repressor is active and shifted to 29°C after eclosion to
787 permit expression of GFP in cells expressing *ase*. At 24 hours post-PTBI (**C-D'''**), but not in control
788 (**A-B'''**) brains, there are GFP+ cells, indicating the expression of *ase*, which is a neural progenitor
789 gene. (**D-D'**). Cells that were Dpn+ (cyan) and PH3+ (red) also were observed in injured brains
790 (**D''-D'''**), but not in controls (**B''-B'''**). *dpn* is a neuroblast and neural progenitor gene. The
791 PH3+Dpn+ cells were often in close proximity to GFP+ cells (**D**), consistent with a lineal
792 relationship.**E-H.** qRT-PCR reveals increases in neural progenitor gene expression following
793 PTBI. The mRNA levels of four different neural progenitor genes were assayed at 4 hours, 24
794 hours, 3 days, 7 days, and 14 days. **E.** The level of *ase* mRNA is increased more than 5-fold by

795 4 hours and remains elevated at 24 hours. However, at 3, 7, and 14 days, *ase* mRNA levels are
796 no longer higher than in controls. **F.** The level of *dpn* mRNA was not detectably increased at any
797 timepoints. **G.** mRNA levels of *erm* are increased almost 3-fold at 4 hours post-injury. However,
798 by 24 hours, 3 days, and 7 days, *erm* mRNA levels have returned to baseline. **H.** *insc* mRNA
799 levels are increased 6-fold at 4 hours, 24 hours, and 3 days post-injury. At later timepoints, 7 and
800 14 days, *insc* mRNA levels return to near baseline. The qRT-PCR results reflect triplicate
801 biological samples, represented relative to the levels of Rp49, and then normalized to the
802 corresponding levels in time-matched controls. Error bars calculated by Relative Expression
803 Software Tool analysis and reflect the standard error of the mean (SEM). Note that scales on Y
804 axes differ among the graphs.
805
806 **Figure 4. Lineage-tracing demonstrates that new neurons are created by Dpn-expressing**
807 **cells.** Using *dpn-Gal4*, the G-TRACE lineage-tracing system (EVANS *et al.* 2009), and a
808 temperature-sensitive Gal80, we lineage-traced *dpn*-expressing cells via their expression of GFP.
809 We observed cells that were GFP+Elav+ (GFP in green; Elav in cyan) at 14 days post-PTBI near
810 the mushroom body (red outlines). The presence of GFP indicates that these cells were either
811 actively expressing or had previously expressed the neuroblast gene *dpn*. GFP+ cells that did
812 not stain with Elav (yellow outlines) also were observed. No GFP+Elav+ cells were observed in
813 age-matched uninjured
814
815 **Figure 5. Perma-twin lineage tracing demonstrates brain regeneration and appropriate**
816 **targeting of axons following PTBI.** To analyze neurogenesis after PTBI, we utilized the perma-
817 twin lineage-tracing system (FERNANDEZ-HERNANDEZ *et al.* 2013). This system permanently labels
818 dividing cells and their progeny with either green fluorescent protein (GFP) or red fluorescent
819 protein (RFP). Flies were reared at 17°C to keep the system off during development. Upon
820 eclosion, F1 males carrying perma-twin transgenes were collected, injured and placed at 30°C to

821 recover for either 2 days or 14 days. **A.** In 2-day uninjured controls, there are some GFP+ cells
822 scattered throughout the brain. **B.** At 14 days, there are relatively few GFP+ cells present in the
823 control central brain. **C.** In comparison, 2-day injured brains have more GFP+ cells that tend to
824 cluster near the injury, (arrowhead). **D.** At 14 days post-injury, there are large clones near the site
825 of injury. Some of these clones have axons that project along the mushroom body tracts
826 (arrowhead). Only the GFP channel is shown here; there were similar RFP+ clones in the PTBI
827 samples. **E.** The number of clones increases over time post-PTBI. Control uninjured brains (n=13)
828 have an average of 10 clones at 2 days while 2-day PTBI brains (n=20) have an average of 23
829 clones ($p<0.00002$). At 7 days, control brains had an average of 9 clones per brain (n=18), while
830 7-day PTBI brains had an average of 39 clones per brain (n=16) (p-value<0.00000002). This is
831 significantly more than the number of clones seen at 2 days post-injury (p-value<0.0009). In 14-
832 day control brains, there are an average of 10 clones per brain, which is not significantly different
833 from the 2-day and 7-day controls. However, at 14 days post-PTBI, there are an average of 66
834 GFP+ clones, which is significantly more than either age-matched controls ($p<0.0000003$) or 2-
835 day post-PTBI brains (p-value<0.0001). Error bars reflect SD. **F-M.** PTBI stimulates clone
836 formation in multiple regions in the brain. Panels on the left side are schematics of brain regions
837 where large clones were found 14 days post-PTBI (**A**, **H**, **J**, **L**). Panels on the right show high
838 magnifications of representative brains (**G**, **I**, **K**, **M**). Many 14-day brains had clones that projected
839 to particular target areas. These included the mushroom body (MB) (**F**, **G**), the ellipsoid body (EB)
840 (**H**, **I**), the antennal lobe (AL) (**J**, **K**), and the lateral horn (LH) (**L**, **M**). **N.** Both clone number and
841 clone size increase with time post-PTBI. The proportions of brain regions with large clones were
842 calculated at 2, 7, and 14 days in controls and injured brains. At 2 days, approximately 8% of
843 control brains (n=13) showed AL clones, while in 2-day injured brains (n=20), there were no AL
844 clones. In 7-day control brains (n=18), 6% had AL and 6% had EB clones. At 7 days post-PTBI
845 (n=16), 6% of brains also had AL clones, 6% had EB clones, and 19% had large MB clones. At
846 14 days, control brains (n=9) did not exhibit any specific areas with clones, while 47% of PTBI

847 brains (n=15) had MB clones, 20% of PTBI brains had AL clones, and 27% of PTBI brains had
848 EB clones, and 27% had LH clones.
849
850 **Figure 6. Locomotor defects observed at 2 days post-PTBI are reversed by 14 days post-**
851 **PTBI.** To assay for functional recovery post-PTBI, we examined locomotor function. The 2 and
852 14 day and age-matched uninjured controls were placed in the *Drosophila* Activity Monitor (DAM)
853 system (TriKinetics, Waltham, MA) to record locomotory behavior. For each condition, 32 newly
854 eclosed males were collected, either injured or kept as uninjured controls, and individually
855 monitored over a 48 hour window. **A.** 2-day control uninjured flies displayed stereotypic
856 locomotory patterns throughout a 24-hour period. However, 2-day post-PTBI flies, exhibited
857 significantly different locomotor profiles (p-value<0.001). **B.** Nonetheless, by 14 days, PTBI flies
858 display comparable locomotor profiles to age-matched controls.
859
860 **Figure 7. Summary model for regeneration following penetrating traumatic brain injury**
861 **(PTBI).** We propose that in young adult *Drosophila* there are quiescent NB-like cells within the
862 central brain that lack expression of canonical NB genes. By 24 hours post-PTBI, the quiescent
863 NB-like cells are activated, express NB genes, and have begun to proliferate. At both 4 hours and
864 24 hours post-PTBI, there is a wave of cell death as assayed using TUNEL. At 7 days, the
865 proliferation rate is still high, and many of the new cells have adopted mature cell identities,
866 becoming neurons or glia. At 10 days post-PTBI, there is no longer a difference in TUNEL+ cells
867 between uninjured brains and injured brains, indicating that the wave of cell death has ended.
868 Because the peaks of both cell death and proliferation occur at the same time post-injury, this
869 could explain why there is not a significant increase in the number of EdU+ cells seen at 7 days
870 compared to the number of PH3+ cells seen at 24 hours. However, by 10 days, cell death is back
871 to control levels while proliferation has decreased but is still slightly above baseline levels. This
872 could explain why there is an increase in the number of EdU+ between 7 and 14 days. At 14 days

873 post-PTBI, there are large clones of new neurons with axons and dendrites correctly projecting to
874 their respective target areas. Locomotor defects are also restored by 14 days, suggesting that
875 adult *Drosophila* are able to regenerate functionally as well as structurally.
876

877 **Supplemental Figure Legends**

878 **Supplemental Figure 1**

879 **S1A. The number of actively dividing cells decreases with time post-injury.** In Fig. 1, we
880 utlilized EdU incorporation at 7 and 14 days to measure cell proliferation. However, EdU labeling
881 is cumulative, allowing one to identify all cells that divided during the labeling period. To obtain
882 snapshots of proliferation in real time, we also carried out PH3 labeling at these same time points
883 post-PTBI. For this experiment, we collected newly eclosed male flies, subjected them to PTBI,
884 and aged them for the specified time periods. We find similar numbers of proliferating cells at 24
885 hours and 7 days post-PTBI, and observe a strong reduction in proliferation at 14 days post-PTBI.
886 At 24 hours, control brains have an average of 3 PH3+ cells (n=11 brains, 28 cells), while PTBI
887 brains have an average of 11 PH3+ cells (n=17 brains, 181 cells). At 7 days, control brains have
888 an average of 2 PH3+ cells (n=6 brains, 11 cells), while PTBI brains have an average of 12 PH3+
889 cells (n=7 brains, 82 cells). At 14 days, control brains have an average of 2 PH3+ cells (n=6
890 brains, 9 cells), while PTBI brains have an average of 4 PH3+ cells (n=6 brains, 24 cells).
891 Unpaired t tests for PTBI to control comparisons at these 3 times points are $p<0.0001$, $p<0.0005$,
892 and $p<0.06$, respectively.

893

894 **S1B. Robust proliferative responses decrease with age.** To explore whether age impacts the
895 amount of cell proliferation that occurs post-injury, we compared newly eclosed adult males to
896 animals aged to 7 days, 14 days, and 28 days prior to PTBI. We then used anti-PH3 to assay cell
897 proliferation 24 hours after injury. Flies injured at within 6 hours of eclosion had an average of 11
898 PH3+ cells/brain (n=17 brains, 182 cells) compared to an average of 3 PH3+ cells/brain in age-
899 matched controls (n=11 brains, 28 cells). Flies that were aged to 7 days, then subjected to PTBI
900 had an average of 6 PH3+ cells/brain (n=11 brains, 65 cells) compared to age-matched controls
901 which had an average of 2 PH3+ cells/brain (n= 5 brains, 12 cells). When flies were aged to 14
902 days prior to PTBI, and assayed 24 hours later, there was an average of 1 PH3+ cell/brain (n=8

903 brains, 11 cells) similar to age-matched controls which also averaged 1 PH3+ cell/brain (n=4
904 brains, 2 cells). 28-day uninjured control (n=4, 1 cell) and PTBI (n=3, 1 cell) flies both averaged 0
905 PH3+cells/brain. Unpaired t tests for PTBI to control comparisons at these 4 time points are
906 $p<0.0001$, $p<0.04$, $p<0.07$, and $p<0.84$, respectively.
907
908 **S1C. Pulse-chase and continuously fed EdU animals have similar numbers of EdU+ cells**
909 **at 7 days post-PTBI.** To assess whether mitotically active cells survive post-PTBI, we used two
910 methods of feeding EdU, pulse-chase (flies are fed EdU for 4 days, then placed on standard sugar
911 food for 3 days) and continuously fed (flies are fed EdU every day before being assayed). At 7
912 days post-PTBI, we find that pulse-chase PTBI brains have an average of 14 EdU+ cells (n=8,
913 108 cells) while continuously fed PTBI brains have an average of 9 EdU+ cells (n=7, 64 cells).
914 Although there is a trend of fewer EdU+ cells in the continuously fed animals, an unpaired t test
915 reveals that this is not significantly different ($p<0.22$). Error bars reflect the standard deviation
916 (SD).
917
918 **S1D. Cell proliferation is not limited to the damaged right hemisphere.** In order to determine
919 where cell proliferation occurs post-PTBI, we counted EdU+ cells in the left and right hemispheres
920 of the central brain. At 7 days, the left hemispheres of control brains have an average of 1 EdU+
921 cells (n=9 brains, 5 cells) while PTBI brains have an average of 4 EdU+ cells (n=15 brains, 63
922 cells; $p<0.04$). In the right hemisphere, control brains have an average of 1 EdU+ cell (n=9 brains,
923 10 cells), while PTBI brains have an average of 7 EdU+ cells (n=15 brains, 109 cells; $p<0.002$).
924 Error bars reflect the standard deviation (SD).
925
926 **S1E. There is no significant difference in the number of PH3+ and EdU+ cells observed 24**
927 **hours post-PTBI.** We use two methods, anti-PH3 immunochemistry to label mitotic cells and
928 EdU labeling of newly synthesized DNA to assay cell division. To assess the extent to which anti-

929 PH3 and EdU labeling are comparable, we evaluated both control and PTBI brains with both
930 methods at 24 hours. We expected to detect more EdU-labeled cells than anti-PH3 labeled cells
931 post-PTBI because anti-PH3 transiently labels cells during M phase of the cell cycle while EdU
932 labeling is cumulative. Instead, we observed similar numbers of labeled cells with the two assays.
933 Specifically, in control brains, there were an average of 3 PH3+ cells (n=11 brains, 28 cells) and
934 2 EdU+ cells (n=6 brains, 13 cells). In PTBI brains, there were an average of 11 PH3+ cells (n=17
935 brains, 181 cells) and 11 EdU+ cells (n=6 brains, 65 cells). Thus, while control and injured brains
936 displayed significant differences in cell proliferation with both assays (PH3: $p<0.0001$, EdU:
937 $p<0.0005$), the number of proliferating cells detected with the two methods was not significantly
938 different. Error bars reflect the standard deviation (SD). There are several potential explanations
939 for this result. For instance, it could be that EdU does not efficiently penetrate the blood brain
940 barrier and/or diffuse through the brain tissue. In this case, only a subset of proliferating cells
941 would be labeled, and EdU labeling would underreport cell proliferation. Alternatively, some of the
942 dividing cells may die. Indeed, DNA synthesis does precede cell death in some contexts (e.g.
943 (RIMKUS *et al.* 2008)). However, the fact that there are similar numbers of EdU positive cells in
944 post-PTBI brains when animals are continuously fed EdU and when they are pulse-chased with
945 EdU (**Fig. S1C**), supports the idea that most dividing cells are viable. It therefore seems likely that
946 EdU does not efficiently penetrate the blood brain barrier and/or diffuse through the brain tissue,
947 particularly in older animals.
948
949 **Supplemental Figure 2**
950 **S2A,B. PTBI decreases lifespan. A.** To assess the impact of PTBI on viability, we performed a
951 lifespan assay with control and PTBI adult male flies. For each condition, >300 flies were assayed.
952 Aging was carried out in vials containing 20-40 flies. Dead flies were counted and surviving flies
953 placed on clean food every 2-3 days. Within the first 12 days, there was no significant difference
954 in survival between control and injured flies. However, beyond 12 days, we saw a significant drop

955 in survival of injured animals. Control males reached 50% survival at 70 days of age, while PTBI
956 males reached 50% survival at 48 days. The maximum lifespan was 84 days for uninjured flies
957 and 74 days for injured flies. This indicates that PTBI does impact lifespan. However, in the
958 window of 0-12 days, there is no significant difference in survival, suggesting that death is more
959 likely due to delayed secondary injury. Error bars reflect the standard deviation (SD). **B.** To test
960 whether age at injury affects outcome, we compared flies injured at 0-6 hours, 14 days, and 28
961 days post-eclosion. Survival was assayed 24 hours later. Control flies at all ages and flies injured
962 0-6 hours post-eclosion, exhibited survival of 98-99% with no significant difference between age-
963 matched control and PTBI flies ($p<0.69$). However, flies injured 14 days post-eclosion showed a
964 significantly reduced survival of 88% ($p<0.0001$), while flies injured 28 days post-eclosion showed
965 a further reduction to 75% survival ($p<0.0001$) compared to age-matched controls. These data
966 indicate that age at the time of PTBI does affect survival. Error bars reflect the standard deviation
967 (SD).
968
969 **S2C-D'. Cell death following PTBI is increased transiently after injury.** To directly test
970 whether PTBI causes cell death, we used terminal deoxynucleotidyl transferase dUTP nick end
971 labeling (TUNEL). TUNEL marks the terminal stages of death, both apoptotic and necrotic, when
972 nuclear DNA has been cleaved and degraded by DNases (GRASL-KRAUPP et al. 1995). We
973 assayed cell death using TUNEL staining (in green) in control and PTBI brains at 4 hours, 24
974 hours and 10 days post-PTBI. DAPI is in blue. We observe a transient increase in cell death. At
975 4 hours post-PTBI, there are an average of 37 TUNEL+ cells/brain (n=5 brains, 183 cells)
976 compared to only 13 TUNEL+ cells/brain (n=5 brains, 67 cells) in uninjured controls. At 24 hours
977 post-PTBI, there are an average of 21 TUNEL+ cells/brain (n=5 brains, 107 cells) compared to
978 only 11 TUNEL+ cells/brain (n=5 brains, 53 cells) in uninjured controls (compare **D** and **D'** to **C**
979 and **C'**). And at 10 days post-PTBI, there are an average of 26 TUNEL+ cells/brain (n=5 brains,
980 132 cells) compared to 24 TUNEL+ cells/brain (n=5 brains, 121 cells) in uninjured controls.

981 Unpaired t tests yield p values of $p<0.003$, $p<0.02$, and $p<0.7$ for the 3 time points, respectively.
982 Error bars reflect the standard deviation (SD). Thus, although the total number of dying cells
983 increases with age in the control brains, cell death due to PTBI appears to peak shortly after the
984 injury such that by 10 days post-injury, there was no significant difference between control and
985 injured brains (**F**).
986
987 **S2E,G,H. PTBI increases neurodegeneration.** To ask whether the observed cell death following
988 PTBI corresponded to neurodegeneration, we used a standardized index (CAO et al. 2013) to
989 analyze histological preparations from brains 25 days after PTBI. Controls exhibited little
990 neurodegeneration at 25 days (**E**). In PTBI flies, we observed an increase in the number of lesions
991 (**G**). Using the neurodegeneration index described in Cao *et al.*, 2013, controls had an average
992 neurodegeneration index score of 1.7+/-0.2, while PTBI flies had an average neurodegeneration
993 index score of 3.0+/-0.4 (**H**). This represented a statistically significant difference ($p<0.01$). Error
994 bars reflect the standard deviation (SD).

Figure 1

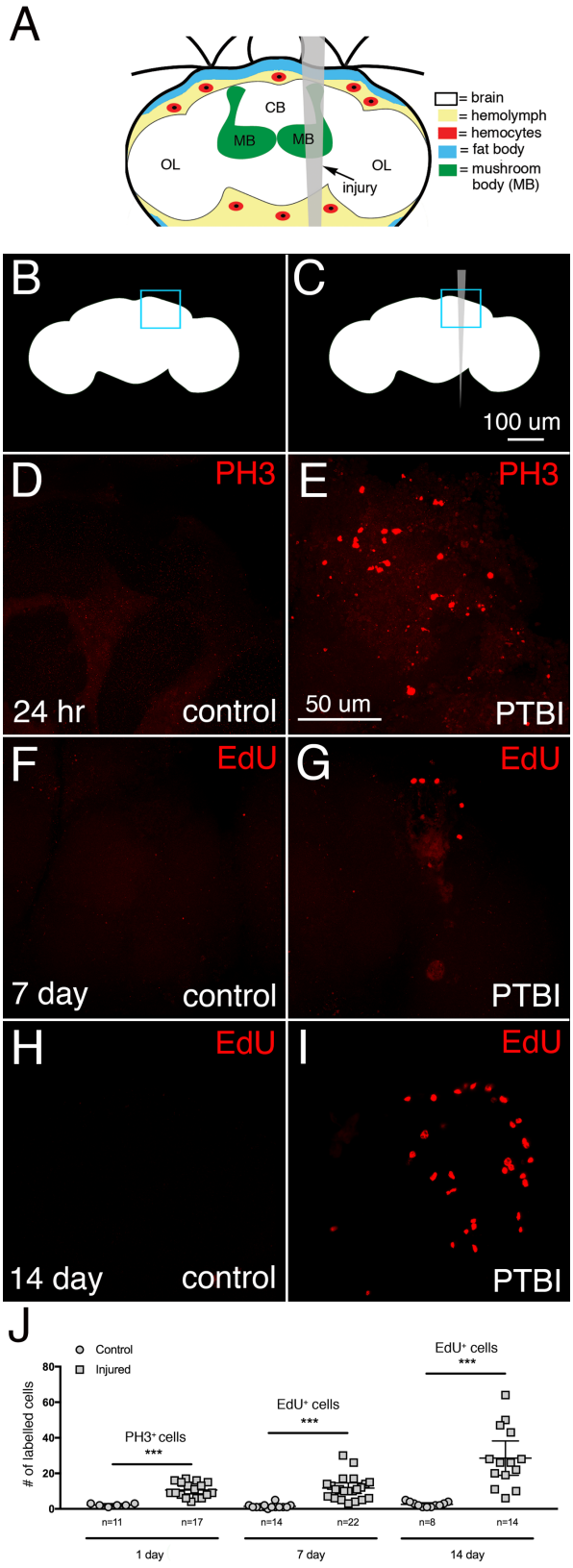
A
CB
MB
MB
OL
OL
injury
= brain
= hemolymph
= hemocytes
= fat body
= mushroom body (MB)
B
C
100 um
D
PH3
24 hr
control
E
PH3
50 um
PTBI
F
EdU
7 day
control
G
EdU
PTBI
H
EdU
14 day
control
I
EdU
PTBI
J
Control
Injured
# of labelled cells
PH3⁺ cells
***
EdU⁺ cells
***
EdU⁺ cells
***
n=11
n=17
n=14
n=22
n=8
n=14
1 day
7 day
14 day

Figure 2

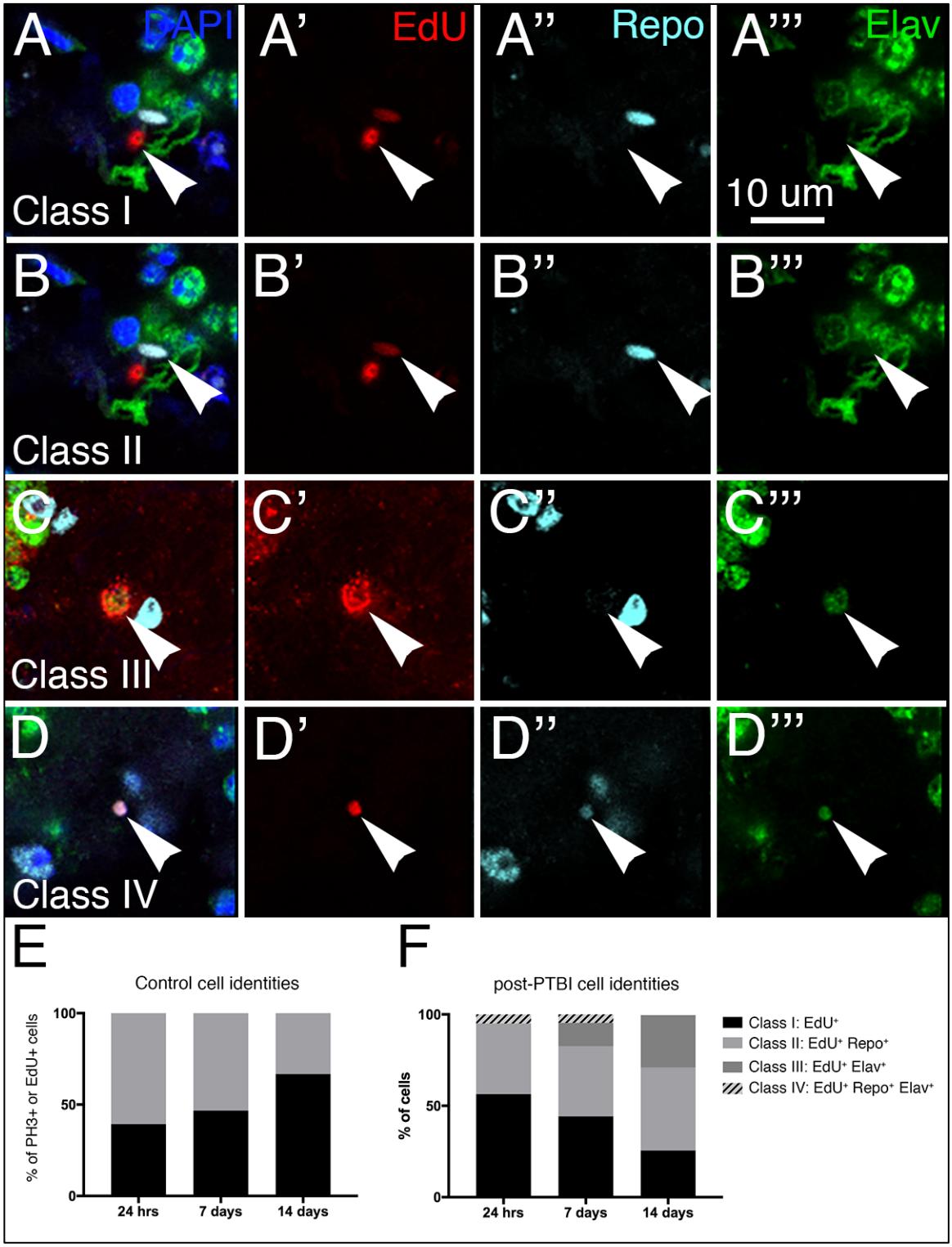
A
DAPI
A'
EdU
A''
Repo
A'''
Elav
Class I
10 um
B
B'
B''
B'''
Class II
C
C'
C''
C'''
Class III
D
D'
D''
D'''
Class IV
E
Control cell identities
% of PH3+ or EdU+ cells
100
50
0
24 hrs
7 days
14 days
F
post-PTBI cell identities
% of cells
100
50
0
24 hrs
7 days
14 days
Class I: EdU+
Class II: EdU+ Repo+
Class III: EdU+ Elav+
Class IV: EdU+ Repo+ Elav+

Figure 3

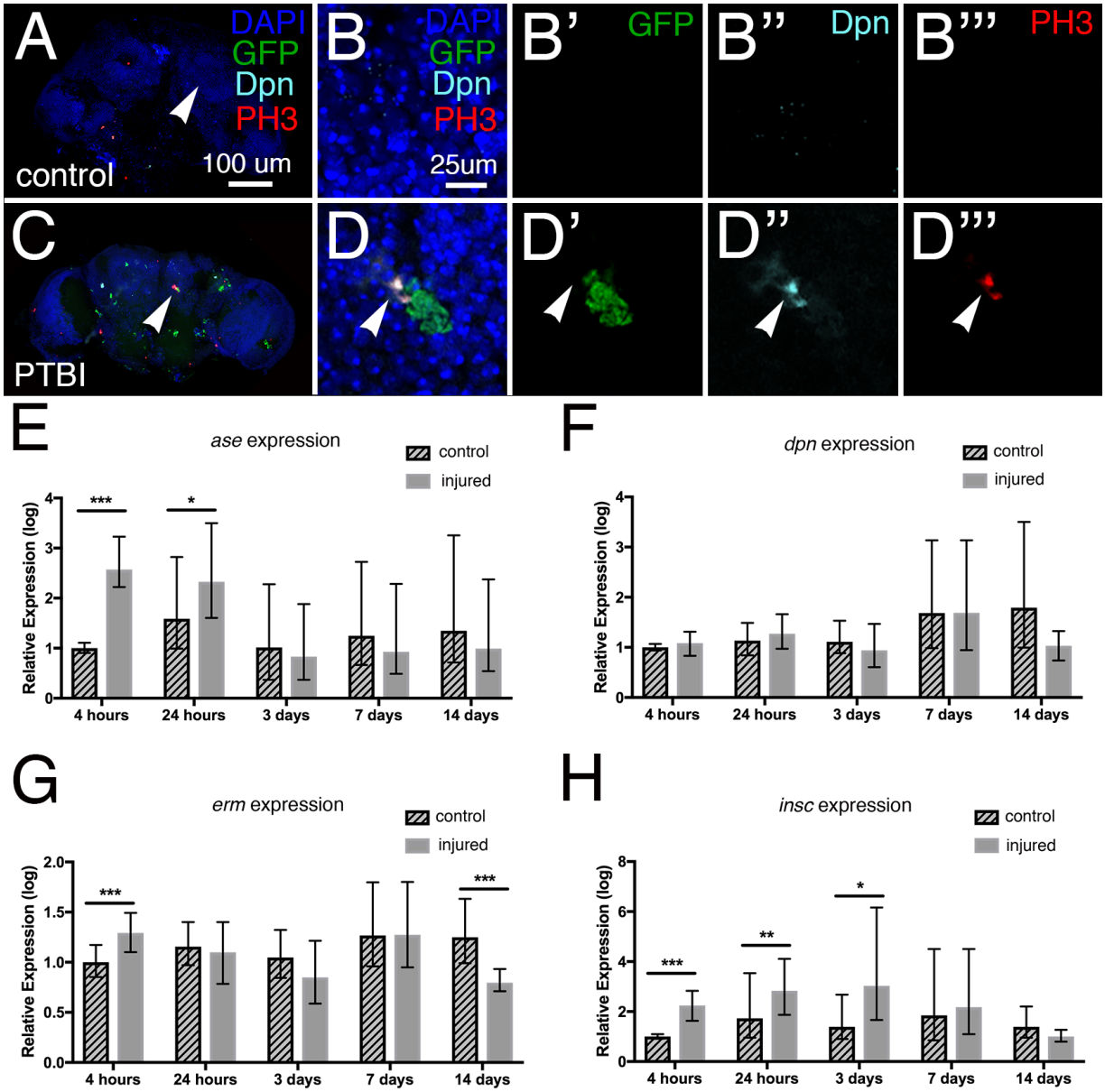
A
DAPI
GFP
Dpn
PH3
control
100 um
B
DAPI
GFP
Dpn
PH3
25um
B'
GFP
B''
Dpn
B'''
PH3
C
PTBI
D
D'
D''
D'''
E
ase expression
control
injured
Relative Expression (log)
4 hours
24 hours
3 days
7 days
14 days
F
dpn expression
control
injured
Relative Expression (log)
4 hours
24 hours
3 days
7 days
14 days
G
erm expression
control
injured
Relative Expression (log)
4 hours
24 hours
3 days
7 days
14 days
H
insc expression
control
injured
Relative Expression (log)
4 hours
24 hours
3 days
7 days
14 days

Figure 4

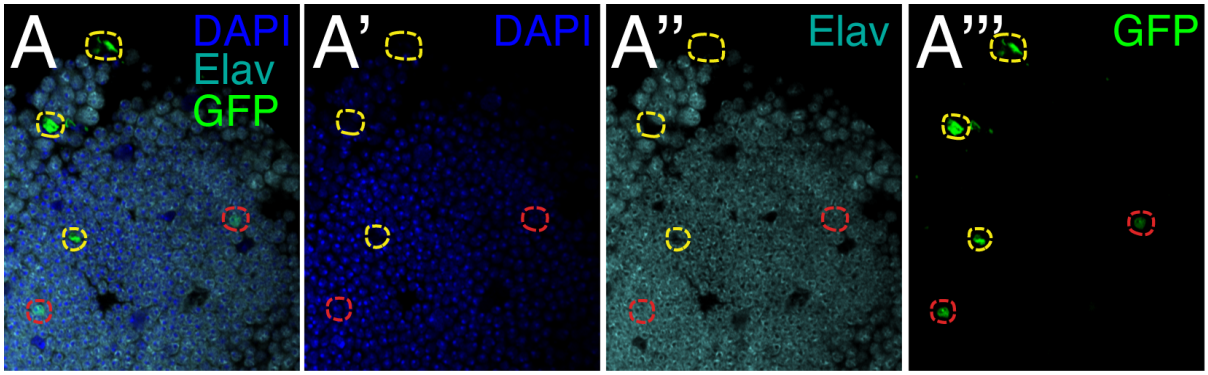

Figure 5

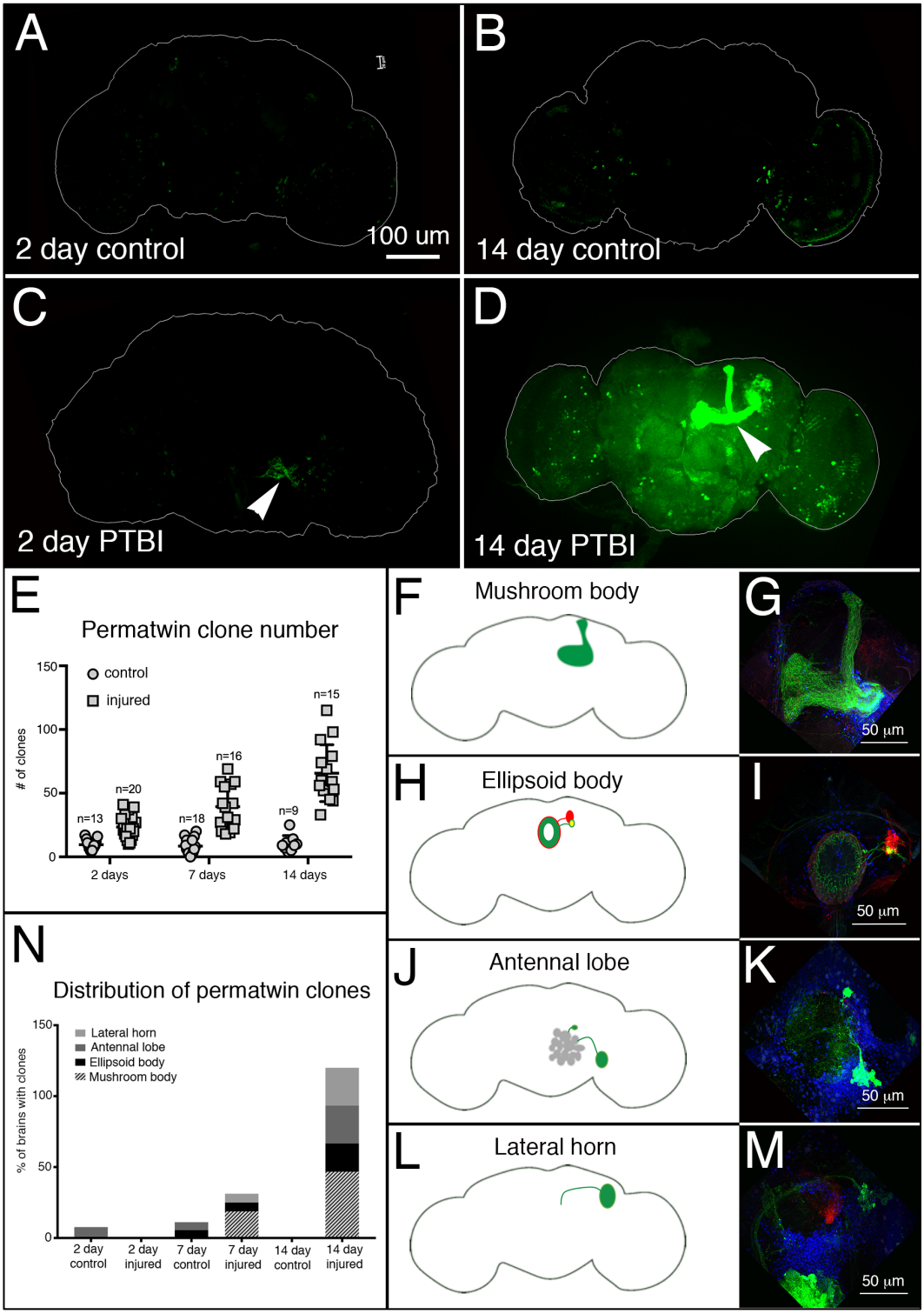
A
2 day control
100 um
B
14 day control
C
2 day PTBI
D
14 day PTBI
E
Permatwin clone number
control
injured
# of clones
150
100
50
0
n=13
n=20
n=18
n=16
n=9
n=15
2 days
7 days
14 days
F
Mushroom body
G
50 µm
H
Ellipsoid body
I
50 µm
J
Antennal lobe
K
50 µm
L
Lateral horn
M
50 µm
N
Distribution of permatwin clones
% of brains with clones
Lateral horn
Antennal lobe
Ellipsoid body
Mushroom body
2 day control
2 day injured
7 day control
7 day injured
14 day control
14 day injured

Figure 6

A

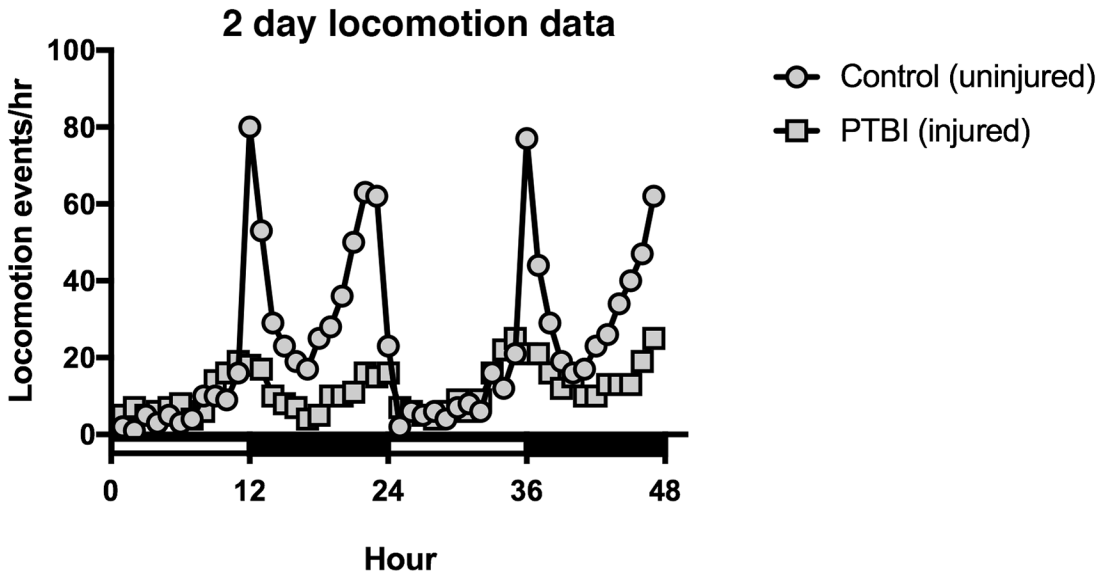
2 day locomotion data
Locomotion events/hr
100
80
60
40
20
0
0
12
24
36
48
Hour
Control (uninjured)
PTBI (injured)

B

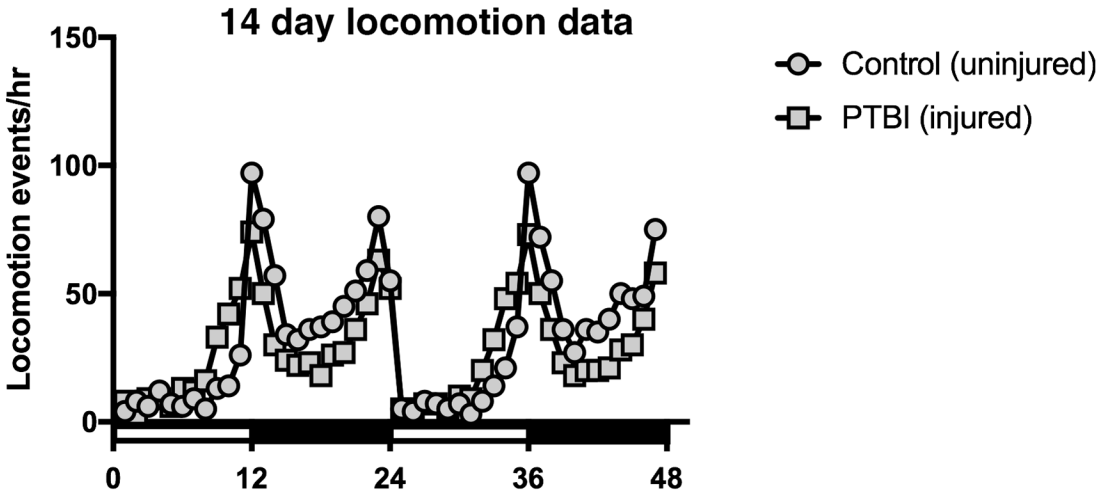
14 day locomotion data
Locomotion events/hr
150
100
50
0
0
12
24
36
48
Control (uninjured)
PTBI (injured)

Figure 7

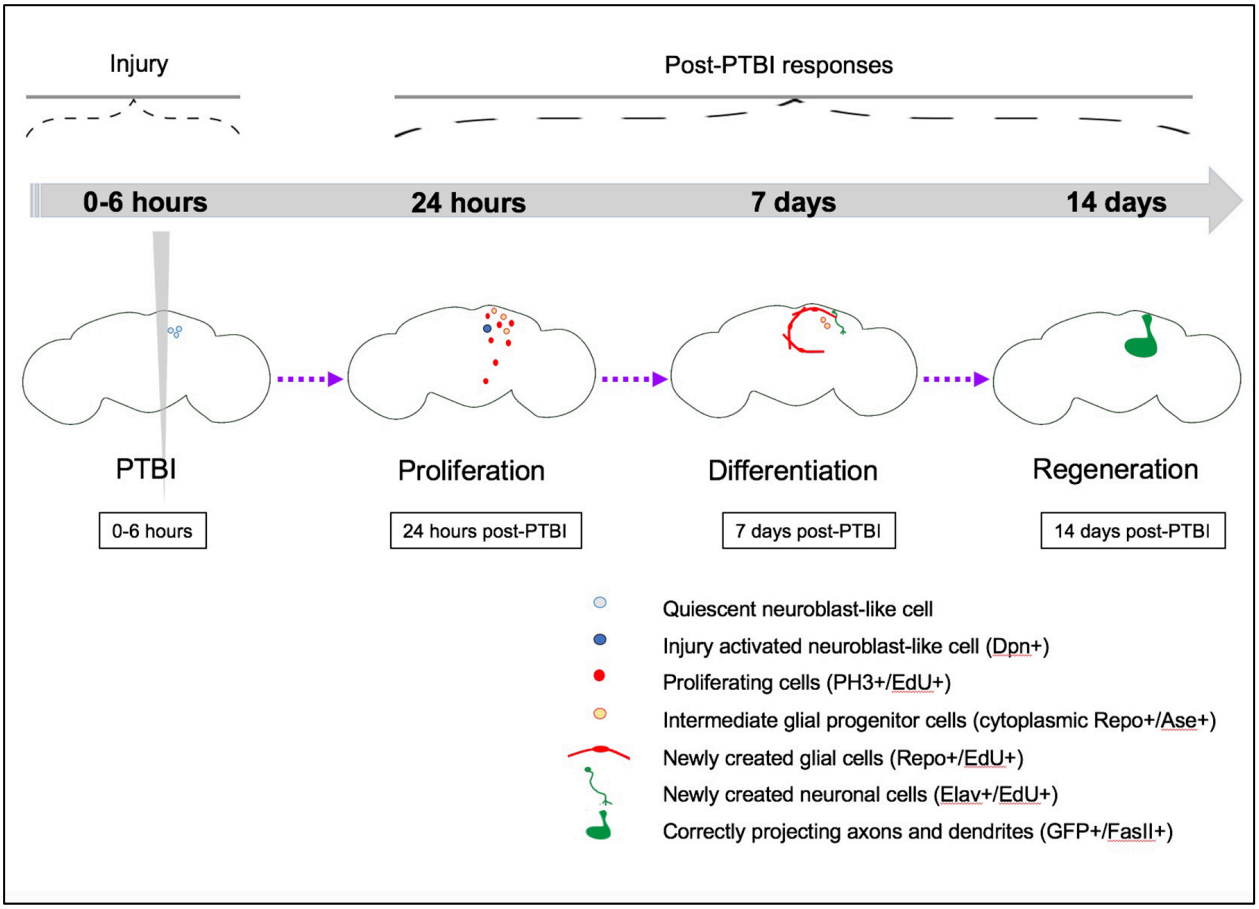
Injury
Post-PTBI responses
0-6 hours
24 hours
7 days
14 days
PTBI
Proliferation
Differentiation
Regeneration
0-6 hours
24 hours post-PTBI
7 days post-PTBI
14 days post-PTBI
Quiescent neuroblast-like cell
Injury activated neuroblast-like cell (Dpn+)
Proliferating cells (PH3+/EdU+)
Intermediate glial progenitor cells (cytoplasmic Repo+/Ase+)
Newly created glial cells (Repo+/EdU+)
Newly created neuronal cells (Elav+/EdU+)
Correctly projecting axons and dendrites (GFP+/FasII+)

Figure S1

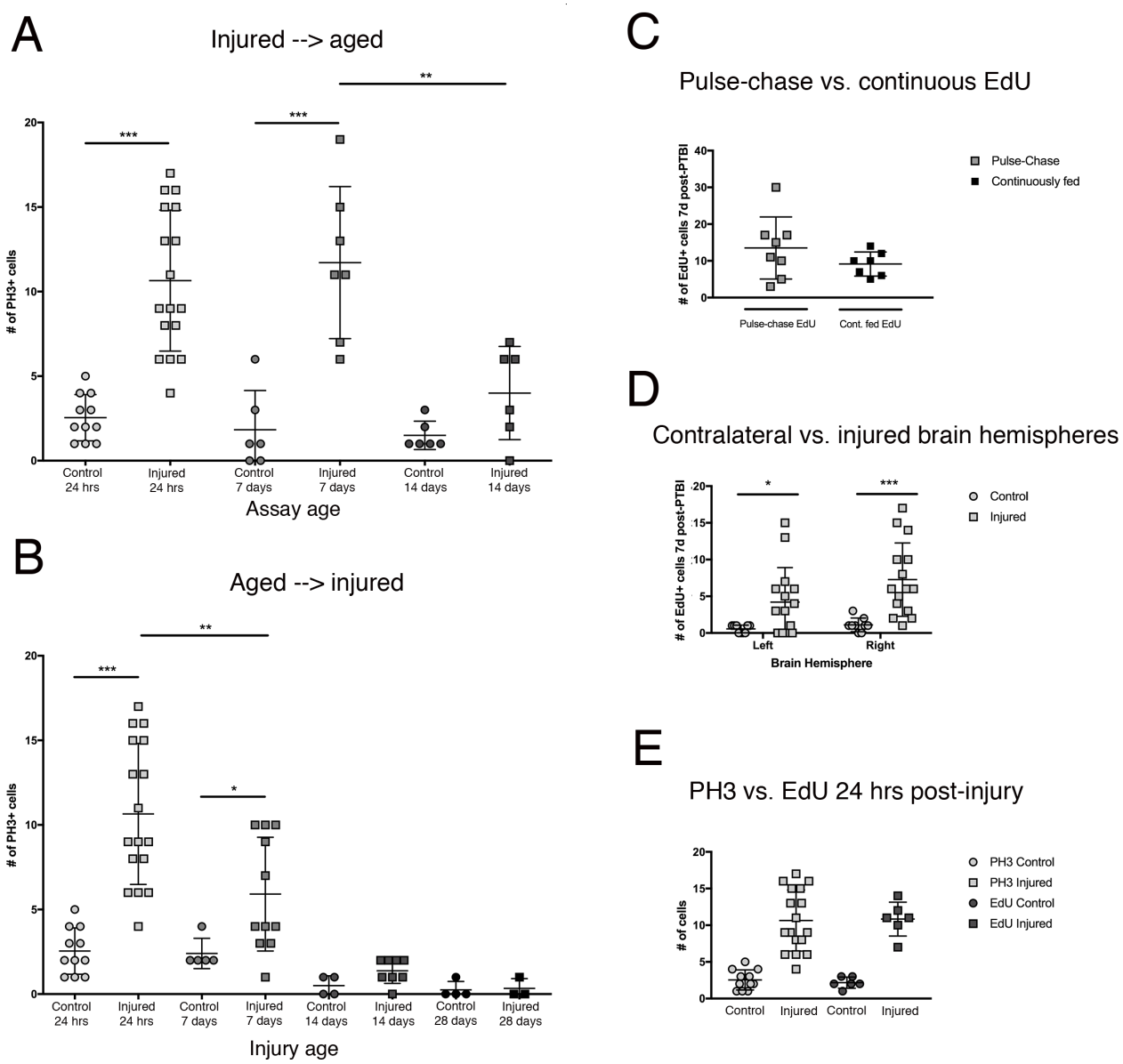
A
Injured --> aged
# of PH3+ cells
Control 24 hrs
Injured 24 hrs
Control 7 days
Injured 7 days
Control 14 days
Injured 14 days
Assay age
B
Aged --> injured
# of PH3+ cells
Control 24 hrs
Injured 24 hrs
Control 7 days
Injured 7 days
Control 14 days
Injured 14 days
Control 28 days
Injured 28 days
Injury age
C
Pulse-chase vs. continuous EdU
# of EdU+ cells 7d post-PTBI
Pulse-chase EdU
Cont. fed EdU
Pulse-Chase
Continuously fed
D
Contralateral vs. injured brain hemispheres
# of EdU+ cells 7d post-PTBI
Left
Right
Brain Hemisphere
Control
Injured
E
PH3 vs. EdU 24 hrs post-injury
# of cells
Control
Injured
Control
Injured
PH3 Control
PH3 Injured
EdU Control
EdU Injured

Figure S2

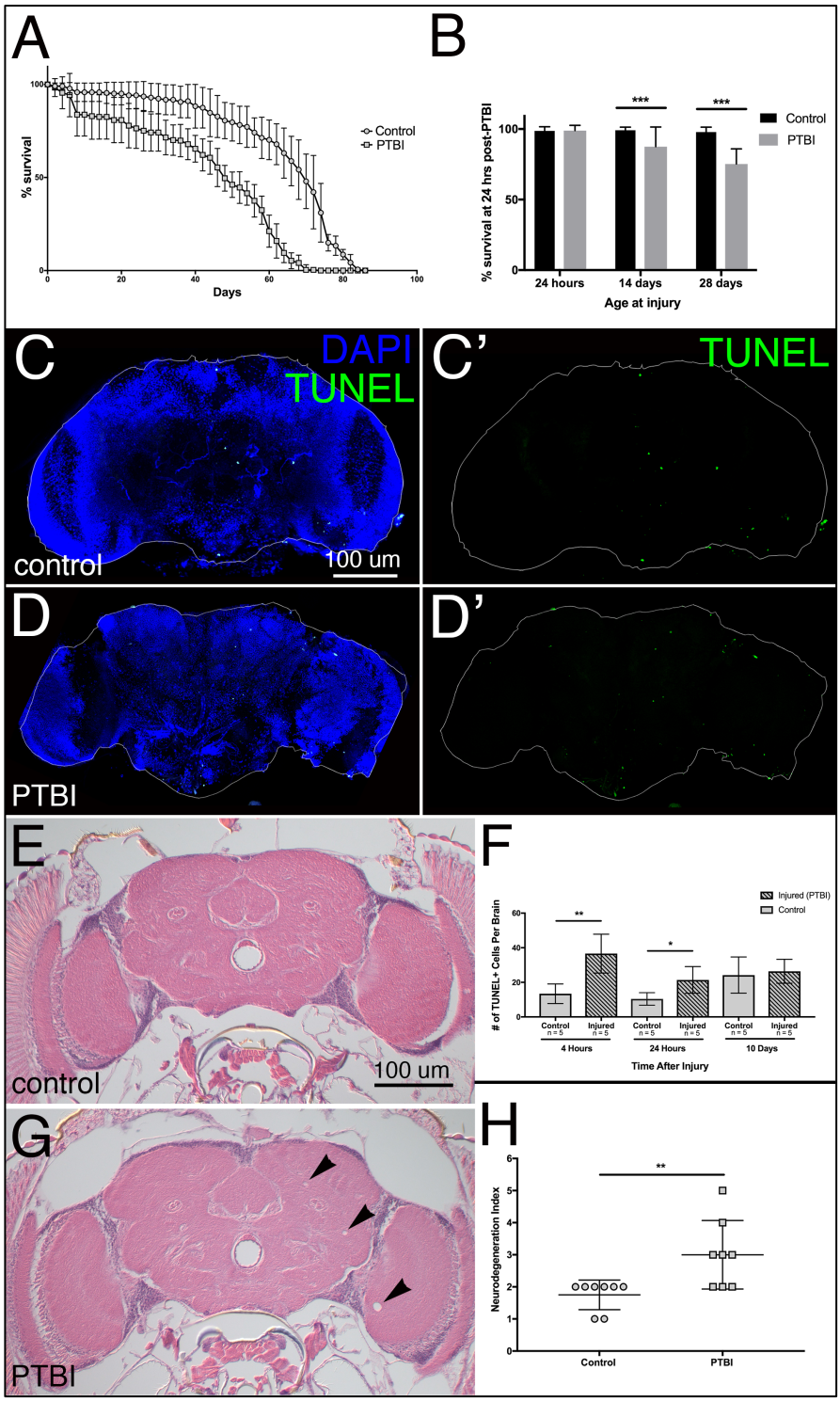
A
% survival
Days
Control
PTBI
B
% survival at 24 hrs post-PTBI
24 hours
14 days
28 days
Age at injury
Control
PTBI
C
DAPI
TUNEL
control
100 um
C'
TUNEL
D
PTBI
D'
E
control
100 um
F
# of TUNEL+ Cells Per Brain
Injured (PTBI)
Control
4 Hours
24 Hours
10 Days
Time After Injury
G
PTBI
H
Neurodegeneration Index
Control
PTBI